Reactivating a positive feedback loop VTA-BLA-NAc circuit associated with positive experience ameliorates the attenuated reward sensitivity induced by chronic stress

Linshan Sun [a,c,1], Jingjing You [a,1], Fengjiao Sun [a,1], Minghu Cui [d], Jiangong Wang [a], Wentao Wang [a], Dan Wang [a], Dunjiang Liu [a], Zhicheng Xu [a], Changyun Qiu [a], Bin Liu [a,*], Haijing Yan [a,b,**]

[a] Institute for Metabolic & Neuropsychiatric Disorders, Binzhou Medical University Hospital, 256603, Binzhou, Shandong, China
[b] Department of Pharmacology, College of Basic Medicine, Binzhou Medical University, 264003, Yantai, Shandong, China
[c] Department of Neurology, Binzhou Medical University Hospital, 256603, Binzhou, Shandong, China
[d] Department of Psychiatry, Binzhou Medical University Hospital, 256603, Binzhou, Shandong, China

ARTICLE INFO

ABSTRACT

Both genetic predisposition and life events, particularly life stress, are thought to increase the risk for depression. Reward sensitivity appears to be attenuated in major depressive disorder (MDD), suggesting deficits in reward processing in these patients. We identified the VTA-BLA-NAc circuit as being activated by sex reward, and the VTA neurons that respond to sex reward are mostly dopaminergic. Acute or chronic reactivation of this circuit ameliorates the reward insensitivity induced by chronic restraint stress. Our histological and electrophysiological results show that the VTA neuron subpopulation responding to restraint stress, predominantly GABAergic neurons, inhibits the responsiveness of VTA dopaminergic neurons to reward stimuli, which is probably the mechanism by which stress modulates the reward processing neural circuits and subsequently disrupts reward-related behaviours. Furthermore, we found that the VTA-BLA-NAc circuit is a positive feedback loop. Blocking the projections from the BLA to the NAc associated with sex reward increases the excitability of VTA GABAergic neurons and decreases the excitability of VTA dopaminergic neurons, while activating this pathway decreases the excitability of VTA GABAergic neurons and increases the excitability of VTA dopaminergic neurons, which may be the cellular mechanism by which the VTA-BLA-NAc circuit associated with sex reward ameliorates the attenuated reward sensitivity induced by chronic stress.

1. Introduction

Depression, one of the world's greatest public health problems, is heterogeneous in aetiology, pathology and treatment response (Garriock et al., 2010; Fabbri et al., 2017). Accumulating evidence strongly supports dysfunction of the brain reward processing system in depression (Bath et al., 2017; Rappaport et al., 2020; Coccurello, 2019). The mesolimbic system, originating from ventral tegmental area (VTA) dopaminergic (DA) neurons that project to the nucleus accumbens (NAc), has been extensively involved in regulating motivated behaviours related to reward stimuli and reward-predictive cues (Halbout et al., 2019;

Ostlund et al., 2014; Wassum et al., 2013), and its abnormalities are associated with deficits in reward-related behaviours (Cao et al., 2010). The VTA-NAc pathway does not regulate reward-related behaviours as an independent brain structure but functions as part of an overlapping and interacting neural circuit. The VTA and NAc receive glutamatergic inputs from the medial prefrontal cortex (mPFC), hippocampus and basolateral amygdala (BLA) (Sesack and Grace, 2010; French and Totterdell, 2003; MacAskill et al., 2012; Britt et al., 2012; Hyman and Malenka, 2001; Nestler and Lüscher, 2019). In return, VTA neurons affect the functions of the mPFC and hippocampus through axonal innervation (Wittmann et al., 2005; Duszkiewicz et al., 2019; Liu et al.,

2018; Popescu et al., 2016). Increasing research suggests that BLA plays an important role in reward processing, particularly in reward learning and goal-directed behaviours (Kim et al., 2016; Wassum and Izquierdo, 2015). Excitatory transmission from the BLA to the NAc increases cue-triggered motivated behaviours and supports positive reinforcement (Gore et al., 2015; Setlow et al., 2002; Stuber et al., 2011). Dopaminergic projections from the VTA to NAc are required for appropriate reward-seeking behaviours regulated by the BLA-NAc pathway (Ambroggi et al., 2008; Stuber et al., 2011). In addition, some neuropharmacological evidence indicates that the VTA may control the activity of the BLA-NAc pathway through axonal innervation of BLA neurons in the addiction process (Di Ciano and Everitt, 2004; Lintas et al., 2011). Nevertheless, further research, especially on the effects on reward processing and on anatomical evidence, is needed to elucidate this neural circuit.

The VTA, a hub of the mesolimbic system that plays an essential role in both reward and aversion (Koob and Le Moal, 2001; de Jong et al., 2019; Russo and Nestler, 2013), is a heterogeneous brain structure containing dopaminergic (65 %), GABAergic (30 %) and glutamatergic (5 %) neurons (Margolis et al., 2006; Nair-Roberts et al., 2008). VTA dopaminergic neurons, the primary focus of research on this brain region, participate not only in processing rewards and reward-predictive cues (Schultz, 2006; Bayer and Glimcher, 2005) but also in responding to aversive and alerting events (de Jong et al., 2019; Bromberg-Martin et al., 2010; Antunes et al., 2020), and abnormalities in the function of VTA dopaminergic neurons are linked to several neuropsychiatric disorders, including addiction, schizophrenia and depression (Willuhn et al., 2010; Guillin et al., 2007; Dunlop and Nemeroff, 2007; Nestler and Carlezon, 2006). It is well established that VTA dopaminergic neurons exhibit rapid and brief burst firing in response to unexpected reward stimuli or reward cues (Pignatelli and Bonci, 2015). Some studies suggest that VTA dopaminergic neurons are inhibited by aversive events (Ungless et al., 2004; Matsumoto and Hikosaka, 2009), while there is

paradoxical evidence showing that VTA dopaminergic neurons are activated by aversive stimuli (Brischoux et al., 2009; Budygin et al., 2012). Recent research has revealed that VTA GABAergic neurons participate in mediating both reward and aversion (Tan et al., 2012; van Zessen et al., 2012) and are strongly modulated by stress (Tan et al., 2012; Ostroumov et al., 2016), indicating a potential role in stress-related neuropsychiatric disorders such as depression and post-traumatic stress disorder (PTSD). Research data have shown that VTA GABAergic neurons synapse onto local VTA dopaminergic neurons and exhibit inhibitory effects on addiction and aversion (Matsui et al., 2014; Matsui and Williams., 2011; Polter et al., 2018; Tan et al., 2012). Despite this knowledge, the role of VTA neurons in normal reward-related behaviours, such as food and sex, remains to be determined, which may help us to better understand the mechanism by which stress induces attenuated reward sensitivity.

2. Results

2.1. Brain areas activated during positive experience

To identify brain regions that are activated during a sexually rewarding experience, we caged male mice with female mice for 2 h (hereafter referred to as a "positive experience") and then performed brain-wide immunofluorescent staining of c-Fos. Histological data showed c-Fos expression in several brain areas, including the basolateral amygdala (BLA), nucleus accumbens (NAc), medial prefrontal cortex (mPFC), ventral tegmental area (VTA), substantia nigra (SN), interpeduncular nucleus (IPN), and dentate gyrus (DG), which have all been implicated in reward processing and motivated behaviours (Zhang et al., 2020; LeGates et al., 2018; Ferenczi et al., 2016; Lammel et al., 2012; Ilango et al., 2014; McLaughlin et al., 2017; Ramirez et al., 2015), in both neutral experience and positive experience mice (Fig. 1A-1 E'). Positive experience mice exhibited more c-Fos-expressing cells in the
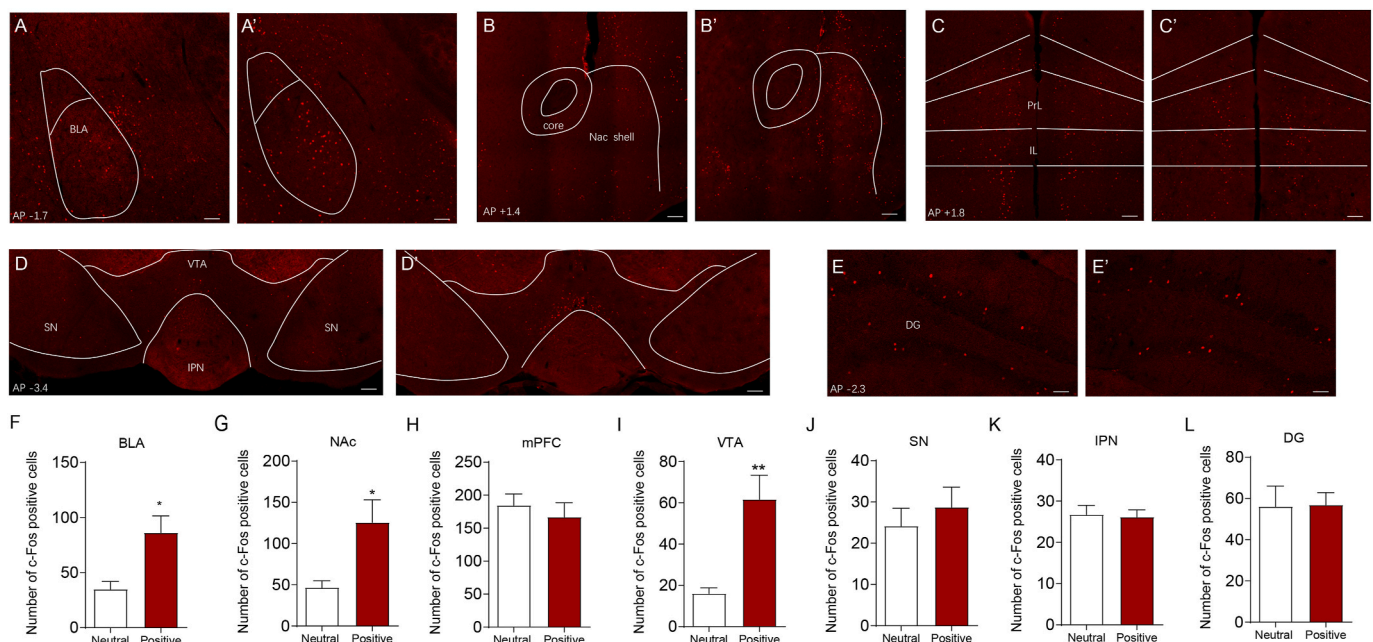

Fig. 1. Positive experience increases c-Fos expression in basolateral amygdala, nucleus accumbens and ventral tegmental area. Whole brain c-Fos staining shows that positive experience (A'-E'), but not neutral experience (A–E), elicits increase of c-Fos expression in basolateral amygdala (BLA) (A, A'), nucleus accumbens (NAc) (B, B'), ventral tegmental area (VTA) (D, D'), but not in the medial prefrontal cortex (mPFC, including prelimbic (PrL) and infralimbic (IL)) (C, C'), substantia nigra (SN) (D, D'), interpeduncular nucleus (IPN) (D, D') or dentate gyrus (DG) (E, E'). Statistical analysis of the histological data revealed a significant increase of c-Fos expression in basolateral amygdala (F, two-tailed unpaired t-test, $t_{(12)} = 2.993$, $P = 0.0112$), nucleus accumbens (G, two-tailed unpaired t-test with Welch's correction, $t_{(7.109)} = 2.747$, $P = 0.0282$) and ventral tegmental area (I, two-tailed unpaired t-test with Welch's correction, $t_{(6.687)} = 3.788$, $P = 0.0074$). Neutral experience group n = 7; positive experience group n = 7. *P < 0.05, **P < 0.01. Data are presented as means±SEM. Annotation (AP): distance from the bregma (mm). Scale bars correspond to 100 μm.

BLA, NAc and VTA (Fig. 1F, G and 1I) but not in the mPFC, SN, IPN or DG (Fig. 1H, J, 1K and L). These results suggest that the VTA, BLA and NAc are activated by positive experiences and may be involved in processing sexual rewards.

2.2. Reactivation of hM3D-labelled VTA neurons during positive experience increases c-Fos expression in the BLA and NAc

The VTA plays a central role in reward processing and motivated behaviours through diverse projections to target brain regions, including the BLA, NAc and mPFC (Lintas et al., 2011; Beier et al., 2015; Pignatelli and Bonci, 2018; Heymann et al., 2020; Hauser et al., 2017; Kumar et al., 2018; Pessiglione et al., 2006). The BLA has a crucial role in cue-triggered motivated behaviours, and its glutamatergic inputs to the NAc have been implicated in reward-seeking behaviours (Ambroggi et al., 2008; Di Ciano and Everitt, 2004; Stuber et al., 2011). A previous pharmacology study indicated that the VTA-BLA-NAc circuit was involved in opiate-related reward processing but did not provide direct and clear anatomical evidence for this circuit (Lintas et al., 2011). We therefore investigated whether the VTA–BLA–NAc circuit was indeed activated during the positive experience. To address this issue, we injected AAV-DIO-hM3D-mCherry into the VTA of Fos-CreER^{T2} mice. Fos-CreER^{T2} mice express the CreER^{T2} fusion protein driven by the endogenous Fos promoter. The Cre-ER^{T2} fusion protein consists of Cre recombinase and a mutant human oestrogen receptor that does not bind its natural ligand (17β-oestradiol) but instead binds the synthetic ligand 4-hydroxytamoxifen (4-OHT). After exposure to 4-OHT, Cre-ER^{T2} entered the nucleus and deleted floxed sequences in Fos-expressing cells. AAV-DIO- hM3D-mCherry contains the coding sequence for the human M3 muscarinic receptor (hM3) with the Y3.33C and A5.46G mutations, which cause it to be insensitive to the endogenous ligand acetylcholine but confer high affinity to clozapine-N-oxide (CNO). When activated by CNO, hM3 enhances neuronal excitability by coupling to Gq-mediated signalling. AAV-DIO-hM3D-mCherry is a Cre-On system with loxP and lox2272 (double-floxed inverted orientation (DIO) (Fig 2P)) in which Cre-mediated inversion of the coding sequence for hM3 is required for its expression. After exposure to conspecific females, Fos-CreER^{T2} male mice were intraperitoneally injected with 4-hydroxytamoxifen (4-OHT, 50 mg/kg) to induce the expression of hM3D-mCherry to label VTA-activated neurons during that positive experience. Three weeks later, we intraperitoneally injected clozapine-N-oxide (CNO, 0.3 mg/kg) to activate previous hM3D-mCherry-labelled VTA neurons (Fig. 2A). Consistent with the increase in c-Fos expression in the VTA (Fig. 1D, D′ and 1I), the positive experience induced an increase in hM3D-mCherry-labelled VTA neurons (Fig. 2B, B′ and 2I). Consequently, there were more c-Fos-positive VTA neurons after intraperitoneal injection of CNO (Fig. 2C, C′ and 2I′). Previous studies showed that VTA neurons could be excited by both rewarding and aversive stimuli (Lintas et al., 2011; Beier et al., 2015; Pignatelli and Bonci, 2018; Heymann et al., 2020). As there might be some alerting cues and aversive stimuli throughout the operation of CNO injection, such as catching mice and intraperitoneal injection, we handled the mice gently to reduce aversive stimuli. Our data showed that the vast majority of the c-Fos-positive VTA neurons were hM3D-mCherry-labelled in both groups (Fig. 2D, D′ and I″, neutral 81.53 ± 5.510 %, positive 86.41 ± 1.888 %), suggesting that VTA c-Fos expression was induced predominantly through activating hM3D by CNO. We next checked c-Fos expression in other brain areas that were activated during the positive experience (Fig. 1). Reactivation of VTA neurons labelled by positive experience correlated with an increase in c-Fos expression in the BLA (Fig. 2E, E′ and 2L) and NAc (Fig. 2F, F′ and M), but not in the SN (Fig. 2C, C′ and 2J), IPN (Fig. 2C, C′ and K), mPFC (Fig. 2G, G′ and 2N), or DG (Fig. 2H, H' and O). Together, these results suggest that the VTA may be upstream of the BLA and NAc during the positive experience.

2.3. VTA-BLA-NAc pathway is activated by positive experience

To verify the hypothetical circuit architecture, i.e., neurons in the VTA synapse onto BLA neurons projecting to specific neurons in the NAc, we injected AAV-WGA-Cre-T2A-ZsGreen and AAV-DIO-mCherry into the VTA and BLA, respectively (Fig 2P). The AAV-WGA-Cre-T2A-ZsGreen virus contains the transsynaptic tracer wheat-germ agglutinin (WGA) fused to Cre recombinase, a ZsGreen reporter, and a linker peptide T2A (2 A peptide derived from insect Thosea asigna virus) whose "self-cleaving" generates two proteins, WGA-Cre and ZsGreen (Hadpech et al., 2018). ZsGreen labels virus-infected VTA neurons (Fig 2Q), and WGA-Cre is released into the synaptic cleft and taken up by adjacent neurons (Libbrecht et al., 2017). WGA-Cre can undergo both anterograde and retrograde transneuronal transfer (Yoshihara et al., 1999; Horowitz et al., 1999) and therefore enter BLA neurons projecting to or receiving inputs from the VTA and induce mCherry expression in AAV-DIO-mCherry-infected BLA neurons (Fig 2R). We observed strong mCherry-positive fibres in the NAc (Fig. 2S) that should be derived from mCherry-labelled BLA neurons receiving inputs from the VTA. These results supported the hypothetical the neural circuit architecture in which neurons in the BLA that synapse onto NAc neurons receive inputs from VTA neurons and indicated that the reactivation of VTA neurons labelled by the positive experience may increase c-Fos expression in the BLA and VTA through the VTA-BLA-NAc pathway but cannot rule out the possibility of increasing c-Fos expression through the VTA- BLA or VTA-NAc pathways.

To address this issue, we performed pseudotyped rabies virus (RABV)-based monosynaptic retrograde tracing (Tervo et al., 2016; Wickersham et al., 2007). AAV-Retro-GFP was injected into the NAc (Fig 2U), which has robust retrograde access to projection neurons, to label projection neurons from the BLA and VTA (Fig 2V and X). C-Fos staining revealed activated neurons in the BLA and NAc during the positive experience (Fig 2V′ and 2X′). The c-Fos-positive BLA neurons were mostly GFP-labelled (Fig 2V″ and 2W, 90.97 ± 1.862 %, n = 4), whereas few c-Fos-positive VTA neurons were GFP-labelled (Fig 2X″ and Y, 11.03 ± 2.189 %, n = 4). Collectively, our data showed that most BLA neurons projecting to the NAc were activated by the positive experience, whereas only a minority of VTA neurons projecting to the NAc were activated, suggesting that the reactivation of VTA neurons previously activated by a positive experience may activate the NAc through the VTA-BLA-NAc pathway.

2.4. Reactivation of VTA neurons previously activated by positive experience rescues chronic restraint stress-induced reward insensitivity

Previous studies suggested that malfunctions of the brain's reward circuits play an important role in mediating stress-elicited reward-related behaviours (Lammel et al., 2014; Kaufling et al., 2017; Bergamini et al., 2018; Robinson et al., 2019). We therefore examined whether reactivation of VTA neurons previously activated during the positive experience could rescue reward insensitivity induced by chronic restraint stress (Fig. 3A). First, Fos-CreER^{T2} mice were injected with AAV-DIO-hM3D-mCherry into the VTA. The mice were assigned to two groups with no significant difference in SPT or FUST (Fig. 3B and C, Basal). The positive experience mice were housed with oestrous female mice for 2 h, and the neutral experience mice were housed with fake toy mice. Then, immediately, all mice received intraperitoneal injection of 4-OHT to allow activity-dependent hM3D-mCherry labelling of the VTA neurons activated by positive experience. The following behavioural experiments were all carried out 45 min after CNO injection. Three weeks later, the SPT showed no difference between the two groups (Fig. 3B, basal CNO), while the FUST showed a significant increase in sniffing time in positive experience mice (Fig. 3C, basal CNO). After 15 days of restraint stress treatment, positive experience mice exhibited a greater sucrose preference (Fig. 3B, Restraint-CNO) and sniffing time (Fig. 3C, Restraint-CNO). The total distance travelled suggested that

there was no significant difference in locomotor activity between the two groups (Fig. 3D). The dose of CNO we used did not influence the behaviours by itself (Supplementary Figs. 1B–1D). These results showed that reactivating VTA neurons that respond to positive experiences could rescue the reward insensitivity induced by chronic restraint stress.

2.5. Distinct subpopulations of VTA neurons activated by positive experience and restraint stress

The VTA is a heterogeneous nucleus including dopaminergic, gamma-aminobutyric acid-ergic (GABAergic), and glutamatergic neurons, in which dopaminergic neurons predominate, making up approximately 55%–65 % of the total neurons (Margolis et al., 2006; Tan et al., 2012; Morales and Margolis, 2017). VTA dopaminergic neurons respond

not only to rewards and reward-predicting stimuli but also to aversion, alerting events and behavioural choices (Bayer and Glimcher, 2005; Brischoux et al., 2009; Dautan et al., 2016; Zhou et al., 2019; Howard et al., 2017). This functional heterogeneity is reflected in the anatomically heterogeneous dopaminergic subpopulations connected with different brain regions (Bromberg-Martin et al., 2010; Engelhard et al., 2019). To clarify the underlying mechanism by which the reactivation of VTA neurons activated by a positive experience ameliorates chronic restraint stress-induced reward insensitivity, we first identified the neuron subpopulation activated during the positive experience. We performed c-Fos staining after the positive experience in DAT-IRES-Cre; Ai14 mice (Fig. 4I), in which tdTomato was exclusively colocalized with the dopaminergic neuron marker TH (97.67 ± 0.7862 %, n = 4) (Fig. 4A–H), confirming that DAT-IRES-Cre-mediated recombination
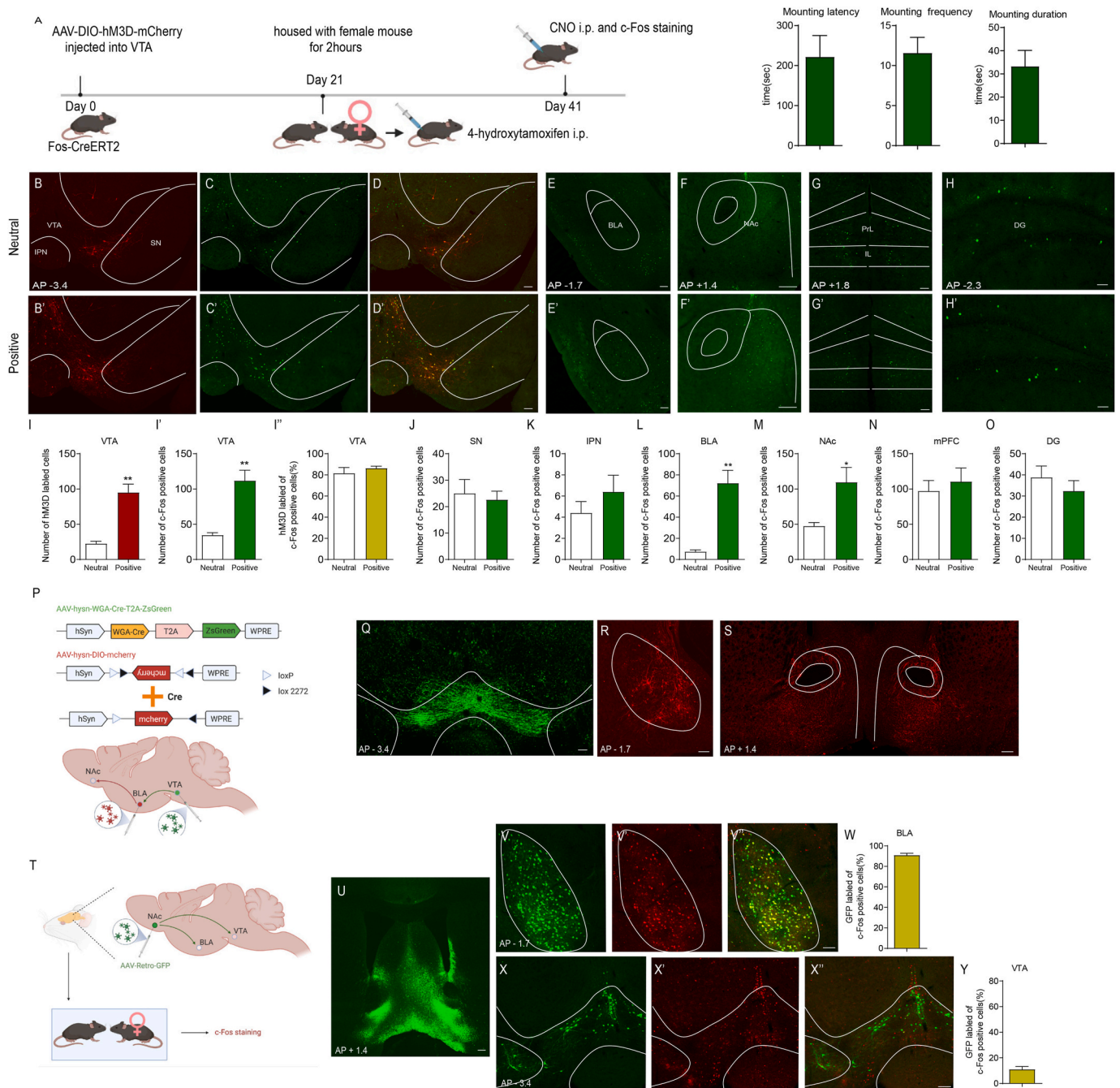
(caption on next page)

Fig. 2. Positive experience activates the VTA-BLA-NAc circuit.
(A) Left, The experimental timeline; Right, sexual behavior, including mounting latency (221.7 ± 53.35, n = 7), mounting frequency (11.57 ± 1.962, n = 7) and mounting duration (33.24 ± 6.888, n = 7). Intraperitoneal injection of 4-OHT induced hM3D-mCherry labeling in activated cells during neutral experience (B) or positive experience (B′) in the VTA, SN and IPN of Fos-CreERT2 mice. Intraperitoneal injection of clozapine-N-oxide (CNO) activated c-Fos expression in hM3D-mCherry-labelled neurons (neutral experience group, C and D; positive experience group, C′ and D′). C-Fos expression in BLA (E, E′), NAc (F, F′), mPFC (G, G′) and DG (H, H′) after reactivating hM3D-mCherry-labelled VTA neurons. Statistical analysis of the histological data revealed that positive experience induced more hM3D-mCherry-labelled VTA neurons compared with neutral experience (I, two-tailed unpaired *t*-test with Welch's correction, t$_{(4.607)}$ = 5.852, P = 0.0027), and that the c-Fos positive VTA cells of positive experience group after CNO injection were more than those of neutral experience group (I′, Mann-Whitney *U* test, P = 0.0079) although most VTA cells were hM3D-mCherry-labelled in both groups (I″, neutral 81.53 ± 5.510 %, positive 86.41 ± 1.888 %). Few cells were labelled with hM3D-mCherry (B, B′) and only a small number of cells were c-Fos-positive after CNO injection (C, C′) in SN and IPN in both groups. Statistical analysis revealed no significant difference in the number of c-Fos-positive cells in SN (J) and IPN (K) between neutral and positive experience groups. The number of c-Fos-positive cells after clozapine-N-oxide injection was significantly different in BLA (L, two-tailed unpaired *t*-test with Welch's correction, t$_{(4.159)}$ = 5.265, P = 0.0056) and NAc (M, two-tailed unpaired *t*-test with Welch's correction, t$_{(4.461)}$ = 2.870, P = 0.04) between neutral and positive experience groups, but not in mPFC (N, Mann-Whitney *U* test, P = 0.5476) and DG (O, two-tailed unpaired *t*-test, t$_{(8)}$ = 0.8750, P = 0.4071). Neutral experience group: n = 5; positive experience group: n = 5. (P) Diagram illustrating virus injection in target areas. (Q) Representative coronal slice showing the expression of AAV-hSyn-WGA-Cre-T2A-ZsGreen (green) 3 weeks after virus injection into the VTA. (R) Representative coronal slice showing the expression of AAV-CAG-DIO-mCherry (red) 3 weeks after virus injection into the BLA. (S) Representative coronal slice showing the strong mCherry–positive (red) fibers in NAc 3 weeks after virus injection into the BLA. (T) Diagram illustrating virus injection in target areas and subsequent positive experience. (U) Representative image showing the injection sites in the NAc. Representative images showing the expression of GFP (V) and c-Fos (V′) in BLA. (V″) Representative image showing c-Fos expression in BLA merged with GFP. (W) Statistical analysis showing the percentage of c-Fos positive BLA neurons that were also GFP labelled (69.81 ± 1.731 %, n = 4). Representative images showing the expression of GFP (X) and c-Fos staining (X′) in NAc. (X″) Representative merged images. (N) Statistical analysis showing the percentage of c-Fos positive VTA neurons that were also GFP labelled (14.25 ± 3.080 %, n = 4). *P < 0.05, **P < 0.01. Data are presented as means±SEM. Annotation (AP): distance from the bregma (mm). Scale bars correspond to 100 μm. . (For interpretation of the references to colour in this figure legend, the reader is referred to the Web version of this article.)

was dopaminergic neuron-specific. Our results showed that VTA c-Fos-positive neurons labelled by positive experience mostly colocalized with tdTomato in DAT-IRES-Cre; Ai14 mice (68.92 ± 4.902 %, n = 5) (Fig. 4J– M), suggesting that the neuron subpopulation that responds to positive experience is predominantly dopaminergic. Dopaminergic neurons maintain the baseline level of dopamine in downstream neural structures through the tonic firing mode and transit to the phasic burst firing mode to induce a sharp increase in dopamine release in response to both rewarding and aversive/stressful stimuli (Di Ciano and Everitt, 2004; Stuber et al., 2011). We therefore next performed in vivo extracellular recording to examine the activity of VTA dopaminergic neurons after the positive experience (Fig 4N) based on the electrophysiological criteria described in previous reports (Tan et al., 2012; Grace and Bunney, 1983; Ungless and Grace, 2012). Consistent with the c-Fos staining results, positive experience increased the number of spontaneously active dopaminergic neurons in the VTA (Fig 4O). The firing rate of spontaneously active dopaminergic neurons was unaffected (Fig 4P), but the percentage of burst firing significantly increased (Fig 4Q). Collectively, these results suggest that the subpopulation of VTA neurons activated during the positive experience are dopaminergic.

We next identified the VTA neuron subpopulation responding to restraint stress. As shown in Fig. 5A–J, restraint stress increased c-Fos expression in the VTA, BLA and NAc. We then performed c-Fos staining in the VTA of DAT-IRES-Cre; Ai14 mice (Fig. 5K), and the results showed that few c-Fos-positive neurons were tdTomato-labelled (17.04 ± 3.513 %, n = 4) (Fig. 5L–O), suggesting that the activated VTA neurons are mostly nondopaminergic, which indicates that the subpopulation of VTA neurons that responds to restraint stress is distinct from the subpopulation that responds to positive experience. To confirm this observation, we detected both restraint stress- and positive experience-activated neurons in similar brain slices of Fos-CreER^{T2} (Fig 5P) and Fos-CreER^{T2}; Ai14 mice (Fig 5U). We injected AAV-DIO-GFP into the VTA of Fos-CreER^{T2} mice, which were subsequently subjected to 2 h of restraint stress and received 4-OHT injection to allow activity-dependent GFP labelling of VTA neurons responding to restraint stress. Three weeks later, we housed these mice with conspecific females and performed c-Fos staining. We observed that the VTA neurons activated by restraint stress (green, Fig 5Q) and positive experience (red, Fig 5R) were anatomically distinct subpopulations (Fig. 5S). Statistical analysis showed that there were few c-Fos-immunopositive VTA neurons labelled by GFP (3.765 ± 1.285 %, n = 5) (Fig 5T). Similar results were observed in Fos-CreER^{T2}; Ai14 mice. The VTA neurons responding to restraint stress (tdTomato, red, Fig 5V) were distinct from those that

responded to the positive experience (c-Fos, green, Fig 5W), and few c-Fos-immunopositive VTA neurons were labelled by tdTomato (3.098 ± 1.412 %, n = 5) (Fig 5X and Y). These results together suggest that the subpopulation of VTA neurons activated by restraint stress is distinct from that activated by positive experience, raising the question of how the VTA neuron subpopulation responding to restraint stress affects reward-related behaviours.

2.6. GABAergic neurons activated by restraint stress inhibit the dopaminergic neurons activated by positive experience

The majority of nondopaminergic VTA cells are GABAergic neurons, which make up approximately 30 % of the total neurons (Dobi et al., 2010). VTA GABAergic neurons have been recognized as potent mediators of reward and aversion, regulating behavioural outputs by projecting to distal brain regions or inhibiting local VTA dopaminergic neurons (van Zessen et al., 2012; Zhou et al., 2019; Bocklisch et al., 2013; Simmons et al., 2017). It has been previously reported that electric footshock activates VTA GABAergic neurons, which inhibit local dopaminergic neurons (Dautan et al., 2016). In our study, the VTA neurons activated by restraint stress were mostly nondopaminergic (Fig 5O), which suggested a possibility that the VTA nondopaminergic cells responding to restraint stress were GABAergic neurons that inhibited the VTA dopaminergic neurons activated by positive experience, subsequently resulting in dysfunctions in reward-seeking behaviours.

To test this possibility, we first identified whether the VTA neurons responding to restraint stress were GABAergic using Vgat-ires-Cre mice. We injected AAV-DIO-mCherry into the VTA of Vgat-ires-Cre mice. As the vesicular GABA amino acid transporter (Vgat) is expressed by GABAergic neurons (Vong et al., 2011), the expression of mCherry is induced in VTA GABAergic neurons. Then, we subjected these mice to 2 h of restraint stress and performed c-Fos staining (Fig. 6A). The results showed that most c-Fos-positive neurons were mCherry-labelled (79.49 ± 3.652 %, n = 5) (Fig. 6B–H), suggesting that the activated VTA neurons were mostly GABAergic. We next performed in vivo extracellular recording to monitor the activity of VTA GABAergic neurons after restraint stress (Fig. 6I) based on the electrophysiological criteria described in previous reports (Tan et al., 2012; Steffensen et al., 1998; Ko et al., 2018). Consistent with the histological results, restraint stress increased the number of spontaneously firing GABAergic neurons (Fig. 6J) but did not influence their firing rate (Fig. 6K), suggesting that the nondopaminergic cells activated by restraint stress are probably GABAergic neurons. Then, we expressed hM3D selectively in VTA
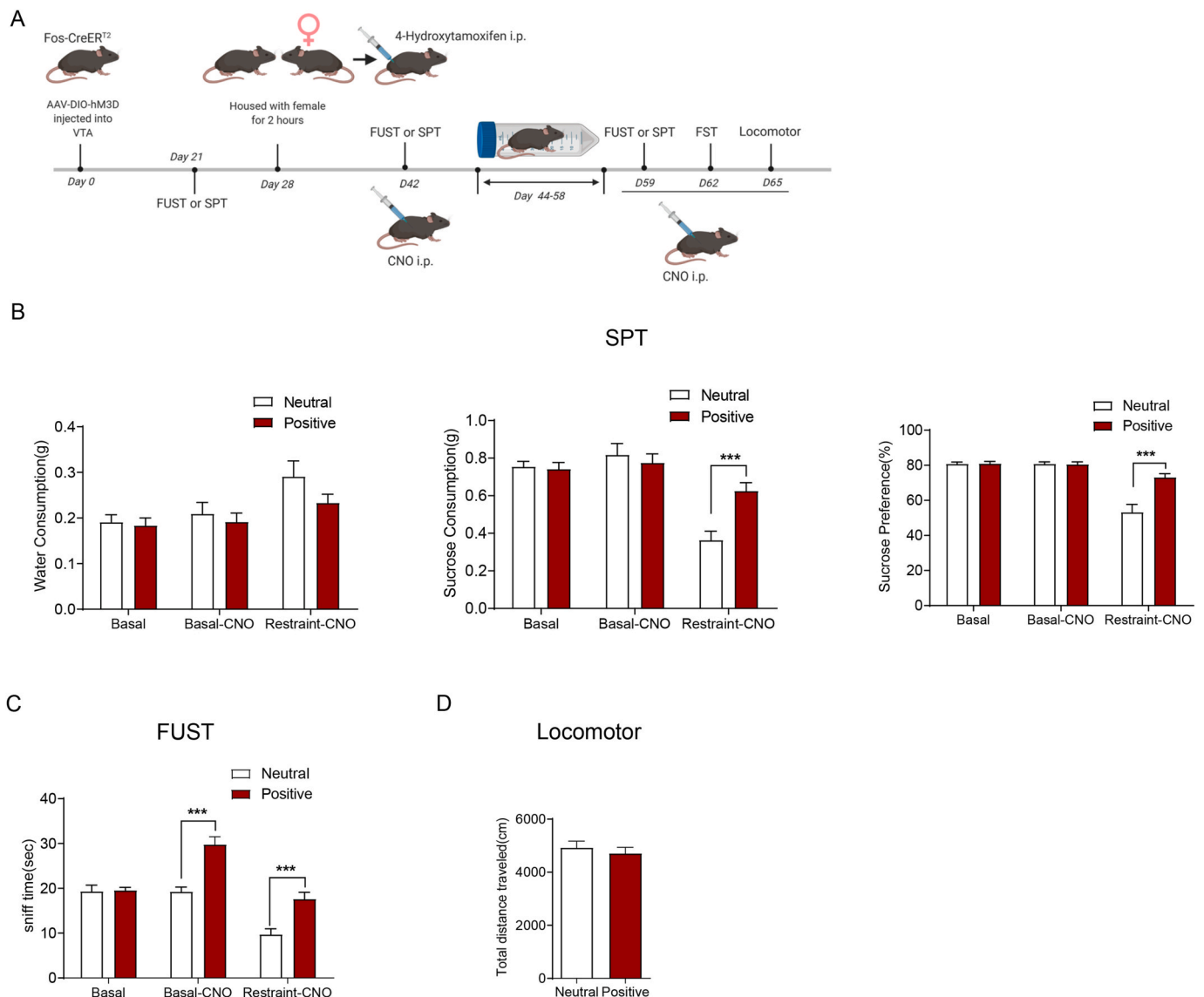
Fig. 3. Acute reactivation of VTA neurons activated by positive experience ameliorates reward insensitivity induced by chronic restraint stress.
(A) The experimental timeline. (B) Sucrose preference test showing reactivation of hm3D-labell
ed VTA neurons during previous positive experience by CNO increased sucrose preference under chronic stress condition. Left, water consumption (subgroups, F (1, 21) = 1.586, P = 0.2218; treatment, F (2, 42) = 8.260, P = 0.0009; subgroups X treatment, F (2, 42) = 0.9042, P = 0.4126; Neutral VS. Positive, Basal P = 0.9932, Basal-CNO P = 0.9273, Restraint-CNO P = 0.2026); Middle, sucrose consumption (subgroups, F (1, 21) = 4.910, P = 0.0379; treatment, F (2, 42) = 22.72, P < 0.001; subgroups X treatment, F (2, 42) = 6.066, P = 0.0048; Neutral VS. Positive, Basal P = 0.9959, Basal-CNO P = 0.8748, Restraint-CNO P = 0.0004); Right, sucrose preference (subgroups, F (1, 21) = 10.09, P = 0.0046; treatment, F (2, 42) = 50.15, P < 0.001; subgroups X treatment, F (2, 42) = 14.20, P < 0.001; Neutral VS. Positive, Basal P = 0.9990, Basal-CNO P = 0.9998, Restraint-CNO P < 0.0001). (C) FUST showing reactivation of hm3D-labelled VTA neurons during previous positive experience by CNO increased sniff time under chronic stress condition (subgroups, F (1, 21) = 37.54, P < 0.001; treatment, F (2,42) = 32.22, P < 0.001; subgroups X treatment, F (2, 42) = 7.818, P = 0.0013; Neutral VS. Positive, Basal P = 0.9989, Basal-CNO P < 0.0001, Restraint-CNO P = 0.0002). (D) There was no significant difference in locomotor activity between two groups (two-tailed unpaired *t*-test, t(21) = 0.6287, P = 0.5364) under chronic stress condition. Neutral experience group n = 11, positive experience group n = 12 in SPT (B), FUST (C), FST (D) and locomotor (E). ***P < 0.001. Data are presented as means±SEM.

neurons that responded to restraint stress by injecting AAV-DIO-hM3D-mCherry (or AAV-DIO-mCherry as a control) into the VTA of Fos-CreER[T2] mice. We subjected these mice to 2 h of restraint stress and immediately intraperitoneally injected 4-OHT to induce the expression of hM3D in activated VTA neurons. We performed in vivo extracellular recording to monitor the activity of VTA dopaminergic neurons in mice exposed to conspecific females 45 min after CNO injection (Fig 6L). Reactivation of the VTA neurons activated by restraint stress decreased the number (Fig 6M) and percentage of burst firing (Fig 6O) in VTA dopaminergic neurons that responded to the positive experience but did not affect their firing rate (Fig 6N). Chronic repeated activation of the VTA neuron subpopulation in response to restraint

stress reduced the excitability of VTA dopaminergic neurons (Fig. 6P–S). The dose of CNO we used did not influence the firing of VTA neurons by itself (Supplementary Figs. 1E–1I). Collectively, our data showed that acute restraint stress increased the activity of VTA GABAergic neurons, which inhibited the activity of VTA dopaminergic neurons responding to positive experiences, and chronic reactivation of the VTA neuron subpopulation responding to restraint stress reduced the excitability of VTA dopaminergic neurons under normal conditions, which may be the underlying mechanism by which chronic stress induces impaired reward-seeking behaviours.
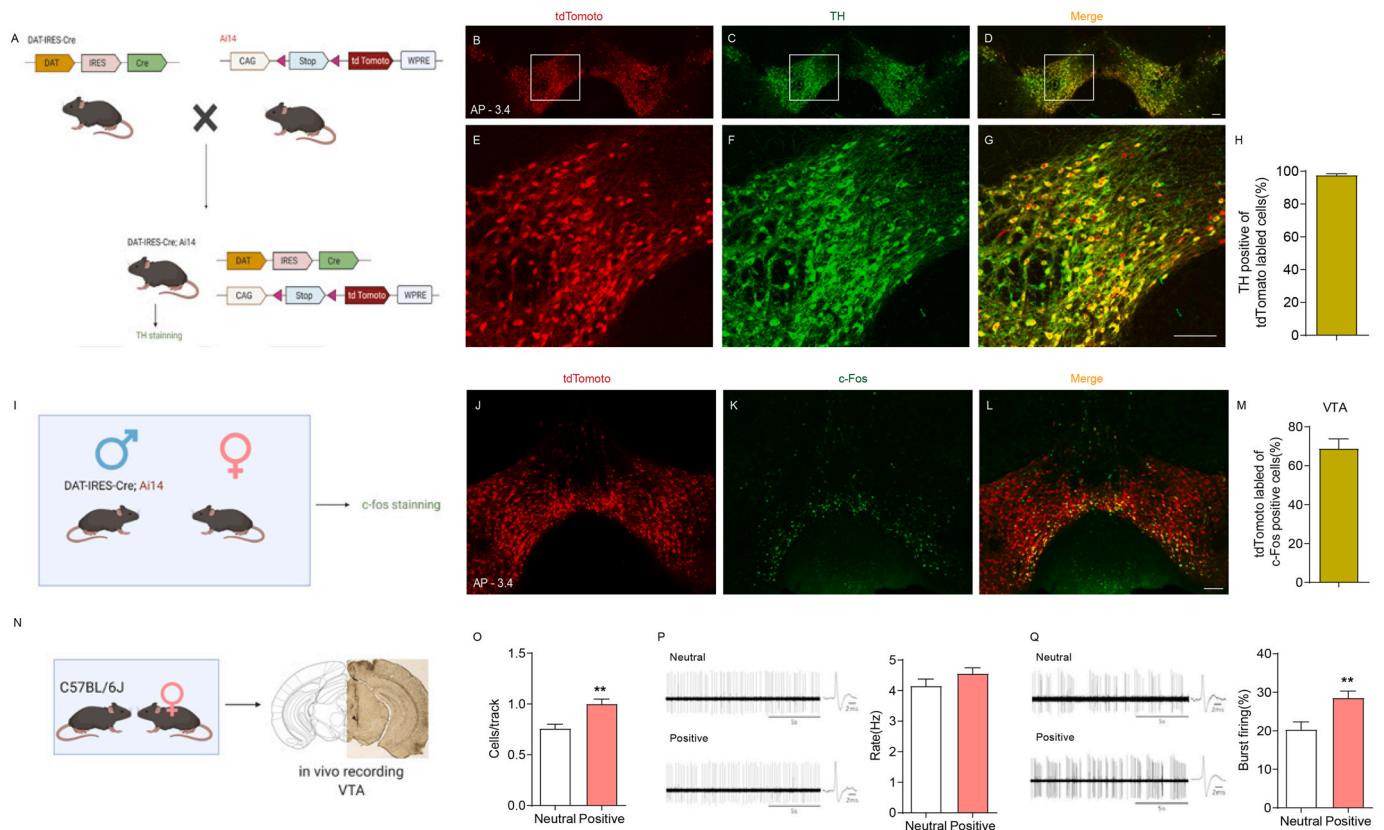
Fig. 4. The activated VTA neurons during positive experience are mostly dopaminergic.
(A) Schematic of the breeding strategy used to generate mice expressing tdTomato specifically in dopaminergic neurons (DAT-IRES-Cre; Ai14). Representative images showing the expression of tdTomato (B, E) and TH staining (C, F) in VTA. (D, G) Images are merged. (H) Statistical analysis showing the percentage of tdTomato-labell

ed VTA neurons positive also for TH (97.64 ± 0.7862 %, n = 4). (I) Schematic showing the experimental procedure for DAT-IRES-Cre; Ai14 mice subject to positive experience and subsequent c-Fos staining. (J) Representative image showing the expression of tdTomato in VTA. (K) Representative image showing the expression of c-Fos in VTA. (L) Images of J and K are merged. (M) Statistical analysis showing the percentage of tdTomato-labelled c-Fos-positive VTA neurons (68.92 ± 4.902 %, n = 5). (N) Diagram showing the experimental procedure and representative image demonstrating the electrode track through the VTA. (O) Positive experience increased the number of spontaneously active dopaminergic neurons per track in the VTA (Mann-Whitney U test, P = 0.0032; Neutral n = 10 mice, Positive n = 9 mice). (P) Left, representative extracellular voltage traces from VTA dopaminergic neurons; Right, statistical result showing the average firing rate of the spontaneously active dopaminergic neurons (two-tailed unpaired t-test, $t_{(17)}$ = 1.331, P = 0.2007; Neutral n = 10 mice (Total 67 neurons), Positive n = 9 mice (Total 81 neurons)). (Q) Left, representative extracellular voltage traces showing the burst firing of VTA dopaminergic neurons; Right, statistical result showing the average percentage of burst firing of the active dopaminergic neurons (two-tailed unpaired t-test, $t_{(17)}$ = 3.063, P = 0.0070; Neutral n = 10 mice (Total 67 neurons), Positive n = 9 mice (Total 81 neurons)). **P < 0.01. Data are presented as means±SEM. Annotation (AP): distance from the bregma (mm). Scale bars correspond to 100 μm.

2.7. Activating the BLA-NAc pathway responsible for positive experience inhibits VTA GABAergic neurons and ameliorates attenuated reward sensitivity

As shown in Fig. 3, acute reactivation of the VTA neurons associated with positive experience ameliorated the attenuated reward sensitivity induced by chronic stress. We wondered whether repeatedly activating the BLA-NAc pathway during the chronic restraint stress procedure could ameliorate the attenuation of reward sensitivity (Fig. 7A). Our data showed that chronic activation of the BLA-NAc pathway associated with positive experience could ameliorate attenuated reward sensitivity, as evaluated by SPT (Fig. 7B), FUST (Fig. 7C), and locomotor activity tests (Fig. 7D). The dose of CNO we used did not influence the behaviours by itself (Supplementary Figs. 2B–2D).

We next explored the cellular mechanism by which activating the BLA-NAc pathway exerted its antidepressant effect. GABAergic medium spiny neurons (MSNs) predominate (approximately 90 %) in the NAc and serve as the only projection neuron (Floresco, 2015). In addition to projecting to the ventral pallidum, NAc MSNs send GABAergic outputs to the VTA (Usuda et al., 1998), which suggests the possibility that the BLA-NAc pathway that responds to positive experience may regulate the

excitability of VTA neurons through GABAergic MSNs sending outputs to the VTA. To test this possibility, we labelled the projections from the BLA to the NAc activated by positive experience with hM4D (mutant human M4 muscarinic receptor) (Fig. 7E) or hM3D (Fig. 7K). After binding to CNO, hM4 couples to Gi and subsequently leads to the attenuation of neuronal firing. Inhibiting the BLA-NAc pathway through the CNO/hM4D system increased the number of spontaneously firing GABAergic neurons (Fig. 7F) and decreased the number of spontaneously firing dopaminergic neurons (Fig. 7H), while activating the BLA-NAc pathway through the CNO/hM3D system decreased the number of spontaneously firing GABAergic neurons (Fig 7L) and increased the number of spontaneously firing dopaminergic neurons (Fig 7N). Neither inhibiting nor activating the BLA-NAc pathway influenced the firing rate of GABAergic neurons (Fig. 7G and M), or the firing rate (Fig. 7I and O) and percentage of burst firing of dopaminergic neurons (Fig. 7J and P). The dose of CNO we used did not influence the behaviours by itself (Supplementary Figs. 2E–2I). Collectively, our data showed that the BLA-NAc pathway associated with positive experience inhibited GABAergic neurons and activated dopaminergic neurons in the VTA, suggesting that activating the BLA-NAc pathway could reverse the influence of chronic stress on the excitability of the GABAergic and
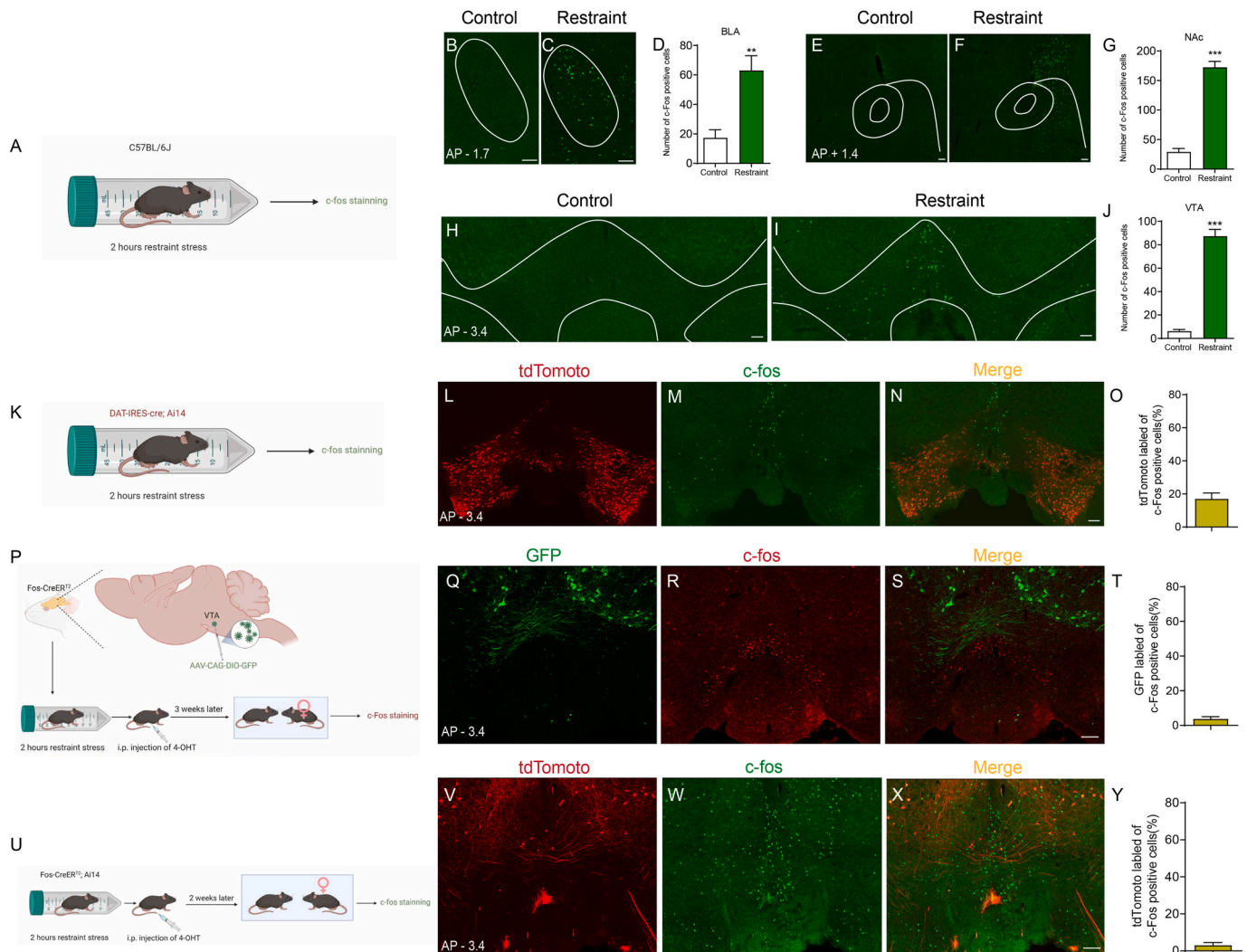
Fig. 5. Positive and negative experiences activate distinct VTA neuron subpopulations.
(A) Schematic showing the experimental procedure for C57BL/6 J mice subject to restraint stress and subsequent c-Fos staining. Representative images showing c-Fos expression in BLA (B and C), NAc (E and F) and VTA (H and I). Statistical analysis showing restraint stress increased c-Fos expression in BLA (D, two-tailed unpaired t-test, $t_{(10)} = 3.989$, P = 0.0026), NAc (G, two-tailed unpaired t-test, $t_{(10)} = 12.23$, P < 0.001) and VTA (J, two-tailed unpaired t-test with Welch's correction, $t_{(5.610)} = 13.69$, P < 0.001). (K) Schematic showing the experimental procedure for DAT-IRES-Cre; Ai14 mice subject to restraint stress and subsequent c-Fos staining. Representative images showing the tdTomato (L) and c-Fos (M) expression in VTA. (N) Images of L and M are merged. (O) Statistical analysis showing the percentage of c-Fos-positive VTA neurons that were labelled by tdTomato (17.04 ± 3.513 %, n = 4). (P) Diagram illustrating virus injection in target areas and subsequent experiments. Representative images showing the GFP (Q) and c-Fos (R) expression in VTA. (S) Images of Q and R are merged. (T) Statistical analysis showing the percentage of c-Fos-positive VTA neurons that were labelled by GFP (3.765 ± 1.285 %, n = 5). (U) Schematic showing the experimental procedure for Fos-CreER[T2]; Ai14 mice. Representative images showing the tdTomato (V) and c-Fos (W) expression in VTA. (X) Images of V and W are merged. (Y) Statistical analysis showing the percentage of c-Fos-positive VTA neurons that were labelled by tdTomato (3.098 ± 1.412 %, n = 5). ***P < 0.001. Data are presented as means±SEM. Annotation (AP): distance from the bregma (mm). Scale bars correspond to 100 μm.

dopaminergic neurons in the VTA, thereby ameliorating attenuated reward sensitivity. Furthermore, our data indicated that the VTA-BLA-NAc circuit responding to positive experience functioned as a positive feedback loop.

3. Discussion

In this study, we used anterograde and retrograde monosynaptic tracing combined with c-Fos immunofluorescence to elucidate the architecture of the VTA-BLA-NAc circuit activated by a sexual reward experience (positive experience). Reactivation of this circuit could ameliorate the reward insensitivity caused by chronic restraint stress. We found that the subpopulation of VTA neurons responding to positive experience was mostly dopaminergic, while the VTA neurons activated by restraint stress belonged to an anatomically distinct cell

subpopulation in which GABAergic neurons predominated and exerted an inhibitory effect on dopaminergic neurons. Furthermore, blocking the projections from the BLA to the NAc resulted in the activation of VTA GABAergic neurons and inhibition of VTA dopaminergic neurons, while activating projections from the BLA to the NAc decreased the excitability of VTA GABAergic neurons and increased the excitability of VTA dopaminergic neurons, suggesting that the VTA-BLA-NAc circuit may function as a positive feedback loop.

The mesocorticolimbic dopaminergic system originating from VTA dopaminergic neurons, which chiefly project to the NAc, BLA, mPFC, and hippocampus, plays an essential role in reward, motivation, cognition, and aversion (Morales and Margolis, 2017; Fields et al., 2007). Its dysfunction has been implicated in many neuropsychiatric disorders, including depression (Vrieze et al., 2013), bipolar disorder (Burdick et al., 2014), schizophrenia (Davis et al., 1991), and addiction

([Koob and Le Moal, 2001](#); [Loureiro and Lüscher, 2018](#)). The VTA-NAc pathway has been extensively studied and is critical for motivation and reward processing ([de Jong et al., 2019](#); [Saddoris et al., 2015](#); [Mohebi et al., 2019](#)), as well as addiction ([Martínez-Rivera et al., 2017](#); [Lüscher, 2016](#)). VTA dopaminergic neurons can facilitate or suppress the target NAc neural activity not only directly through dopaminergic receptors residing on NAc neurons ([Soares-Cunha et al., 2016](#); [Pascoli et al., 2015](#)) but also by regulating excitatory glutamatergic inputs to

NAc neurons originating from the BLA via presynaptic mechanisms ([Stuber et al., 2011](#); [Charara and Grace, 2003](#)), integrating different inputs and turning them into action via outputs to the ventral pallidum ([Creed et al., 2016](#)) and lateral hypothalamus ([Luo et al., 2018](#); [Maldonado-Irizarry et al., 1995](#)). In our study, positive experience significantly increased active VTA, BLA and NAc neurons ([Fig. 1](#)), and reactivation of the VTA neurons activated by positive experience could enhance the neural activity of BLA and NAc ([Fig. 2](#)A–O), suggesting that
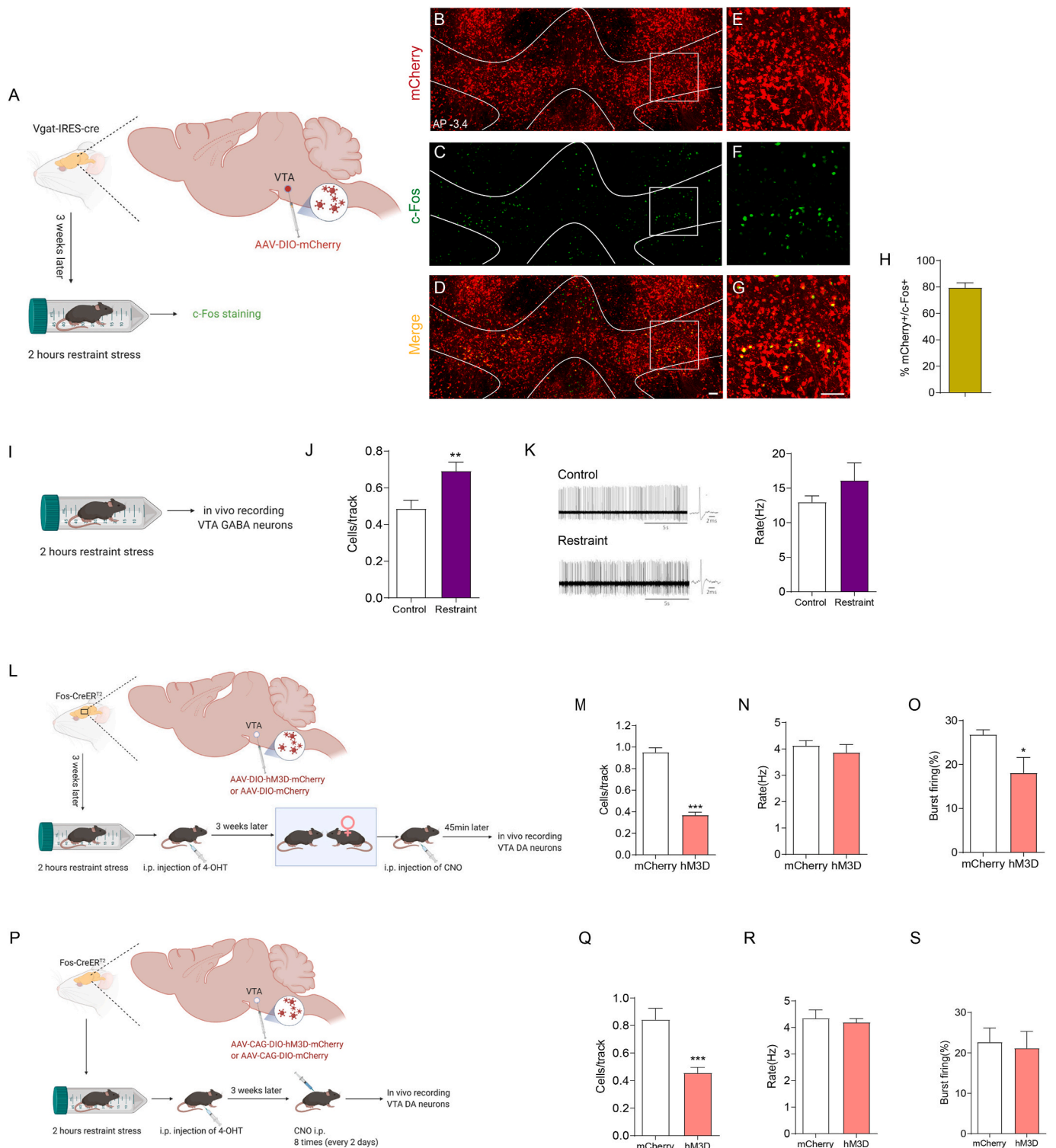
(caption on next page)

Fig. 6. **The VTA GABAergic neurons activated by restraint stress inhibit local VTA dopaminergic neurons responding to positive experience**.
(A) Diagram illustrating virus injection in target areas and subsequent experiments. Representative images showing the expression of mCherry (B, E) and c-Fos staining (C, F) in VTA. (D, G) Images are merged. (H) Statistical analysis showing the percentage of mCherry -labelled VTA neurons positive also for c-Fos (79.49 ± 3.652 %, n = 5). (I) Schematic showing the experimental procedure for C57BL/6 J mice subject to restraint stress and subsequent in vivo extracellular recording. (J) Restraint stress increased the number of spontaneously active GABAergic neurons per track in the VTA (Mann-Whitney *U* test, P = 0.0089; C ontrol n = 8 mice (35 neurons), Restraint n = 9 mice (56 neurons)). (K) Left, representative extracellular voltage traces from VTA GABAergic neurons; Right, statistical result showing the average firing rate of the active GABAergic neurons (two-tailed unpaired *t*-test with Welch's correction, $t_{(9.995)}$ = 1.173, P = 0.2679; Control n = 8 mice (35 neurons), Restraint n = 9 mice (56 neurons)). (L) Diagram illustrating virus injection in target areas and subsequent experiments. Reactivation of VTA neurons previously activated by restraint stress inhibited the responsiveness of VTA dopaminergic neurons to sexual reward, decreasing the number of spontaneously active dopaminergic neurons per track in the VTA (M, Mann-Whitney *U* test, P < 0.0001; mCherry n = 7 mice (60 neurons), hM3D n = 9 mice (30 neurons)) and the percentage of burst firing (O, two-tailed unpaired *t*-test with Welch's correction, $t_{(9.443)}$ = 2.370, P = 0.0406; mCherry n = 7 mice (60 neurons), hM3D n = 9 mice (30 neurons)), but no change in the firing rate (N, two-tailed unpaired *t*-test, $t_{(14)}$ = 0.6785,P = 0.5085; mCherry n = 7 (60 neurons), hM3D n = 9 mice (30 neurons)). (P) Diagram illustrating virus injection in target areas and subsequent experiments. Chronic reactivation of VTA neurons previously activated by restraint stress decreased the number of spontaneously active dopaminergic neurons per track in the VTA (Q, Mann-Whitney *U* test, P = 0.0002; mCherry n = 9 mice (67 neurons), hM3D n = 10 mice (42 neurons)), but no change in the firing rate (R, two-tailed unpaired *t*-test, $t_{(17)}$ = 0.2940, P = 0.7723; mCherry n = 9 mice (67 neurons), hM3D n = 10 mice (42 neurons)) and the percentage of burst firing (S, two-tailed unpaired *t*-test, $t_{(17)}$ = 0.5666, P = 0.5784; mCherry n = 9 mice (67 neurons), hM3D n = 10 mice (42 neurons)), under normal condition. *P < 0.05, **P < 0.01, ***P < 0.001. Data are presented as means±SEM. Annotation (AP): distance from the bregma (mm). Scale bars correspond to 100 μm.

BLA and NAc were target nuclei of VTA during the positive experience. The results obtained from the c-Fos staining experiment combined with retrograde tracing showed that almost all BLA neurons activated by the positive experience synapsed onto the NAc (Fig 2V″), while only a few activated VTA neurons projected to the NAc (Fig 2X″), suggesting that the reactivation of VTA neurons activated by positive experience increased NAc neural activity, probably through activating BLA neurons projecting to the NAc. There is some evidence obtained from neuropharmacological experiments indicating that the VTA-BLA-NAc neural circuit is involved in modulating rewarding effects and motivated behaviours (Di Ciano and Everitt, 2004; Lintas et al., 2011), but direct anatomical evidence is still lacking. We determined the putative neuronal circuit using WGA-Cre transsynaptic tracing technology (Librecht et al., 2017; Hadpech et al., 2018), and the results showed that mCherry-labelled BLA neurons received inputs from the VTA and sent projections to the NAc (Fig. 2P–S), providing neuroanatomical evidence for the VTA-BLA-NAc circuit.

Dysfunction of the brain reward processing system has been implicated in neuropsychiatric disorders such as bipolar disorder (Caseras et al., 2013), schizophrenia (Strauss and Gold, 2012) and depression (Nestler and Carlezon, 2006; Pizzagalli et al., 2009). The present medication treatments for depression, with the view that depression is a general brain dysfunction, take weeks to alleviate depressive symptomatology, and approximately 30 % of patients obtain little improvement and are defined as having treatment-resistant depression (TRD) (Akil et al., 2018; Fogelson and Leuchter, 2017). More focused, targeted treatments that modulate specific brain networks or areas, such as deep brain stimulation (DBS), may prove to be promising approaches to help treatment-resistant patients (Kiening and Sartorius, 2013; Mayberg et al., 2005; Dandekar et al., 2018). A recent study by Steve Ramirez and his colleagues demonstrated that activating DG cells associated with positive memory could alleviate chronic stress-induced behavioural impairments (Ramirez et al., 2015). We therefore investigated whether directly activating the neural circuitry responsible for reward processing during positive experiences could ameliorate depression-like behaviours induced by chronic restraint stress. We found that reactivating the VTA neurons associated with positive experience through the CNO/hM3D system could ameliorate the reward insensitivity induced by chronic restraint stress (Fig. 3).

VTA dopaminergic neurons mediate a diverse array of functions associated with distinct axonal targets, including reward-related learning, goal-directed behavior, working memory, and decision making (Morales and Margolis, 2017; Björklund and Dunnett, 2007; Baimel et al., 2017). They exhibit rapid burst firing in response to rewarding stimuli or rewarding cues, sharply increasing dopamine release to their target brain regions (Pignatelli and Bonci, 2015; Lohani et al., 2018; Lavin et al., 2005). In our study, the VTA neurons activated by positive

experience were mostly dopaminergic, and their burst firing increased (Fig. 4). Some studies have shown that VTA dopaminergic neurons are also excited by aversive stimuli (Bromberg-Martin et al., 2010; Brischoux et al., 2009; Budygin et al., 2012), while there are paradoxical reports that they are inhibited by aversive events (Ungless et al., 2004; Matsumoto and Hikosaka, 2009). Recently, increasing evidence suggests that GABAergic neurons of the VTA, the majority of VTA nondopaminergic neurons, are involved in mediating reward and aversion (Tan et al., 2012; van Zessen et al., 2012; Eshel et al., 2015). In our study, c-Fos staining revealed that restraint stress also induced neuron activation in the VTA, BLA and NAc (Fig. 5A–J), but the activated VTA neurons were mostly nondopaminergic (Fig. 5K–O). Consistent with a previous report that aversive stimulus activated VTA GABAergic neurons (Tan et al., 2012), our histological and electrophysiological results showed that restraint stress increased the number of spontaneously active GABAergic neurons in the VTA (Fig. 6A–K), indicating that the activated nondopaminergic neurons were probably GABAergic. Our data suggested that the VTA may process reward and aversive stimuli through dopaminergic and GABAergic neurons, respectively. Given the difference in VTA neuron types responding to restraint stress and sexual reward, how restraint stress influences the performance of reward-seeking behaviours is unknown (Fig. 3). Our results revealed the distinct anatomical locations of these two VTA neuron subpopulations (Fig. 5P–Y), but we noticed that the restraint stress-responsive neurons sent fibres to the anatomic location of positive experience-responding neurons, indicating that there may be synaptic connections between these distinct neuron subpopulations. It is generally accepted that VTA GABAergic neurons promote aversive behaviours by inhibiting VTA dopaminergic neurons (Tan et al., 2012; Bocklisch et al., 2013), prompting us to determine whether VTA neurons activated by restraint stress inhibit the responsiveness of VTA dopaminergic neurons to positive experiences. The positive experience increased the number of active dopaminergic neurons and the percentage of burst firing neurons (Fig. 4N–Q), which was inhibited by the reactivation of VTA neurons activated by restraint stress (Fig. 6L–O). Repeatedly activating the VTA neuron subpopulation that responds to restraint stress reduced the excitability of the VTA dopaminergic neurons (Fig. 6P–S), which may be the underlying mechanism by which chronic stress induces impaired reward-seeking behaviours. Our data were consistent with those in a previous study by Ruud van Zessen and his colleagues, which showed that nonspecific activation of the VTA GABA neurons reduced the excitability of neighbouring VTA dopaminergic neurons in vitro (van Zessen et al., 2012), while our work specifically targeted the VTA neuron subpopulation responding to restraint stress and provided electrophysiological evidence in vivo.

Previous studies have shown that NAc MSNs send GABAergic feedback projections to the VTA (Floresco, 2015; Sesack and Grace, 2010).

Yang et al. showed that MSNs in the NAc could directly inhibit dopaminergic neurons in the VTA or indirectly activate dopaminergic neurons by inhibiting VTA GABAergic interneurons (Yang et al., 2018). In this study, we found that the reactivation of projections from the BLA to NAc was responsible for the sex reward as it resulted in the activation of dopaminergic neurons and inhibition of GABAergic neurons in the VTA (Fig. 7K– P). In summary, we propose a putative positive feedback loop composed of the VTA, BLA and NAc. A subpopulation of VTA dopaminergic neurons is activated during sex rewards. BLA cells are activated by VTA dopaminergic neurons and subsequently increase the activity of a subset of NAc MSNs projecting to VTA GABAergic neurons, inhibiting the excitability of their target VTA GABAergic neurons and the release of VTA dopaminergic neurons from inhibitory controls. This positive feedback loop may be the underlying mechanism by which activating the VTA-BLA-NAc circuit rescues the reward insensitivity induced by chronic stress (Fig. 7A-D).

In conclusion, we uncovered a novel positive feedback loop, the VTA-BLA-NAc circuit, that is activated by positive experience and inhibited by VTA GABAergic neurons responding to stress. Reactivation of this circuit can ameliorate the reward insensitivity induced by chronic restraint stress.

4. Materials and methods

4.1. Animals

C57BL/6 mice were purchased from the Pengyue Laboratory of China, and transgenic mice (DAT-IRES-Cre, 006660; Ai14, 007908; Fos-
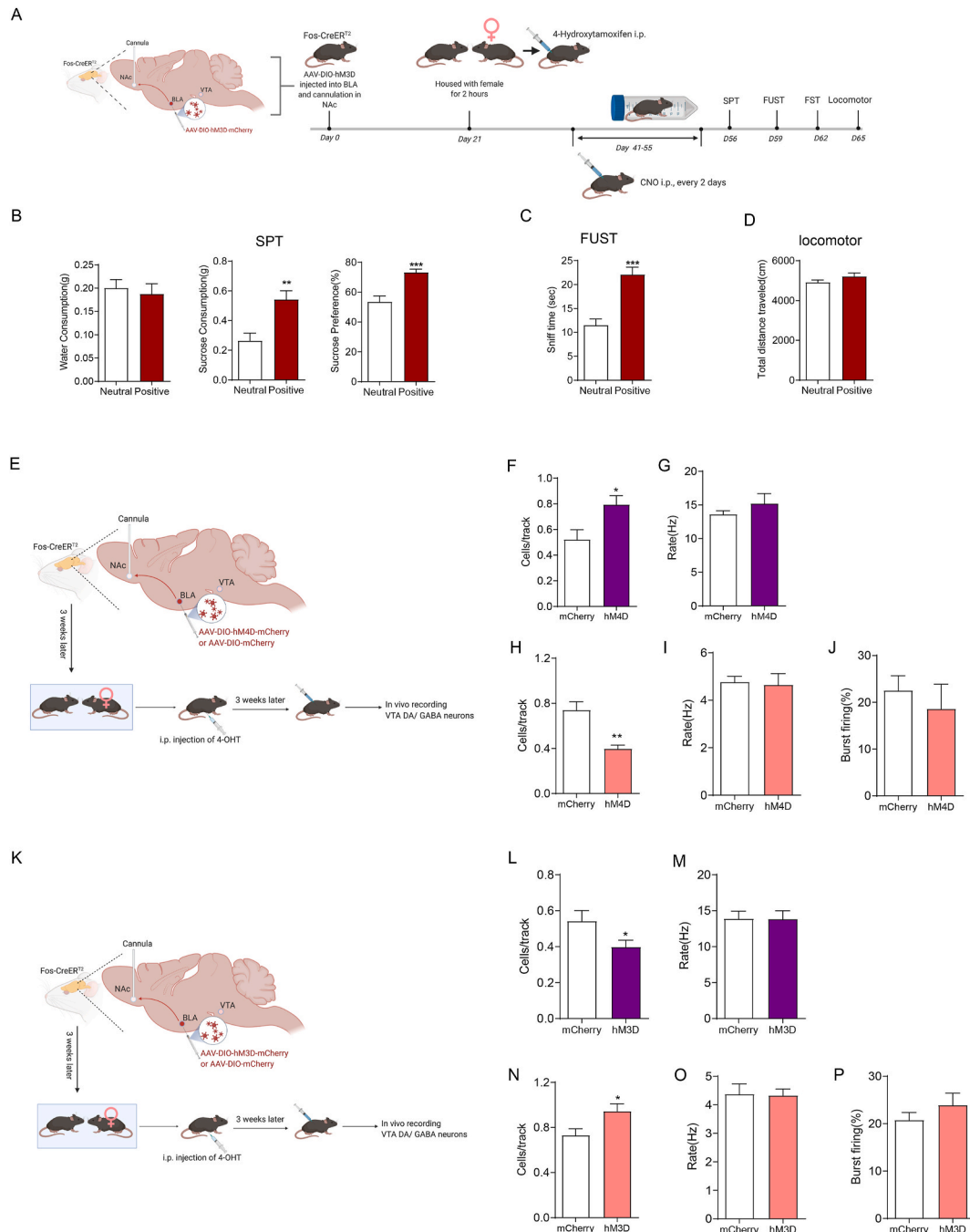
(caption on next page)

Fig. 7. Chronic reactivation of the BLA-NAc circuit responding to positive experience rescues attenuated reward sensitivity induced by chronic restraint stress.
(A) Diagram illustrating virus injection and implanting cannula in target areas and subsequent experiments. (B) Chronic reactivation of projections from BLA to NAc specially activated during positive experience by infusion of CNO into NAc increased sucrose preference under chronic stress condition. Left, water consumption (Mann-Whitney U test, P = 0.3531); Middle, sucrose consumption (two-tailed unpaired t-test, $t_{(20)}$ = 3.451, P = 0.0025); Right, sucrose preference (wo-tailed unpaired t-test, $t_{(20)}$ = 4.624, P = 0.0002). Chronic reactivation of projections from BLA to NAc specially activated during positive experience increased female urine sniff time (C, two-tailed unpaired t-test, $t_{(20)}$ = 5.117, P < 0.0001), but did not influence the locomotor activity between two groups (D, two-tailed unpaired t-test, $t_{(21)}$ = 1.353, P = 0.1911), under chronic stress condition. Neutral experience group n = 10, positive experience group n = 12 in SPT (B), FUST (C), and locomotor (D). (E) Diagram illustrating virus injection and implanting cannula in target areas and subsequent experiments. Blockade of the projections from BLA to NAc responding to positive experience by CNO infusion increased the number of spontaneously active GABAergic neurons per track in the VTA (F, two-tailed unpaired t-test, $t_{(14)}$ = 2.616, P = 0.0203; mCherry n = 8 mice (37 neurons), hM4D n = 8 mice (50 neurons)), didn't influence the firing rate (G, two-tailed unpaired t-test with Welch's correction, $t_{(8.766)}$ = 1.004, P = 0.3423: mCherry n = 8 mice (37 neurons), hM4D n = 8 mice (50 neurons)), while decreased the number of spontaneously active the dopaminergic neurons per track in the VTA (H, Mann-Whitney U test, P = 0.0023; mCherry n = 6 mice (40 neurons), hM4D n = 7 mice (24 neurons)) and no change in the firing rate (I, two-tailed unpaired t-test, $t_{(11)}$ = 0.2173, P = 0.8320; mCherry n = 6 mice (40 neurons), hM4D n = 7 mice (24 neurons)) and the percentage of burst firing (J, two-tailed unpaired t-test, $t_{(11)}$ = 0.6126, P = 0.5526; mCherry n = 6 mice (40 neurons), hM4D n = 7 mice (24 neurons)). (K) Diagram illustrating virus injection and implanting cannula in target areas and subsequent experiments. Reactivation of the projections from BLA to NAc responding to positive experience by CNO infusion decreased the number of spontaneously active GABAergic neurons per track in the VTA (L, two-tailed unpaired t-test, $t_{(16)}$ = 2.146, P = 0.0476; mCherry n = 8 mice (39 neurons), hM3D n = 10 mice (36 neurons)), didn't influence the firing rate (M, two-tailed unpaired t-test, $t_{(16)}$ = 0.02529, P = 0.9801: mCherry n = 8 mice (39 neurons), hM3D n = 10 mice (36 neurons)), while increased the number of spontaneously active the dopaminergic neurons per track in the VTA (N, two-tailed unpaired t-test, $t_{(13)}$ = 2.386, P = 0.0330: mCherry n = 7 mice (46 neurons), hM3D n = 8 mice (68 neurons)) and no change in the firing rate (O, two-tailed unpaired t-test, $t_{(13)}$ = 0.1097, P = 0.9143; mCherry n = 7 mice (46 neurons), hM3D n = 8 mice (68 neurons)) and the percentage of burst firing (P, Mann-Whitney U test, P = 0.5358; mCherry n = 7 mice (46 neurons), hM3D n = 8 mice (68 neurons)). *P < 0.05, **P < 0.01, ***P < 0.001. Data are presented as means±SEM.

CreER^{T2}, 021,882; Vgat-IRES-Cre, 016,962) were purchased from the Jackson Laboratories. The protocols of the animal studies were approved by the Institutional Animal Care and Use Committee of Binzhou Medical University Hospital and performed in compliance with the National Institutes of Health Guide for the Care and Use of Laboratory Animals. Efforts were made to minimize animal suffering and the number of animals used.

4.2. AAV virus

AAV2/9-hSyn-DIO-hm3D (Gq)-mCherry (in the main text referred to as AAV-DIO-hm3D-mCherry), AAV2/9-hSyn-DIO-hm4D (Gi)-mCherry (in the main text referred to as AAV-DIO-hm4D-mCherry), AAV2/9-hsyn-DIO-mCherry (in the main text referred to as AAV-DIO-mCherry), AAV2/9-CAG-mCherry (in the main text referred to as AAV-CAG-mCherry), AAV2/9-hsyn-WGA-Cre-T2A- ZsGreen (in the main text referred to as AAV-hSyn-WGA-Cre-T2A-ZsGreen), AAV2-CAG-Retro-GFP (in the main text referred to as AAV-Retro-GFP) were purchased from Shanghai Hanheng Biotechnology, China.

4.3. Drugs

Clozapine-N-oxide (CNO) was purchased from Sigma, dissolved in saline at a concentration of 0.5 mg/ml and diluted in saline to a final concentration of 0.03 mg/ml (hM3D) for intraperitoneal injection. For intra-NAc microinjection (hM4D), CNO was diluted in saline to a final concentration of 3 mM. 4-Hydroxytamoxifen (4-OHT) was purchased from Sigma and dissolved in ethanol. Corn oil (Sigma) was added to the 4-OHT solution, which was shaken and mixed at 37 °C, put in a fume hood for ethanol volatilization to a final concentration of 5 mg/ml and stored at −20 °C with protection from light.

4.4. Stereotaxic surgery

For microinjection of AAV virus, mice were anaesthetized and mounted onto a stereotaxic frame (KOPF, USA). AAV virus was injected with a glass pipette using an infusion pump (Micro 4, WPI, USA). Viruses were injected bilaterally into target brain areas using the following co-ordinates: VTA, AP = −3.30 mm, ML = ± 0.50 mm, DV = −4.20 mm, from bregma; flow rate of 0.10 μl/min and total volume of 1.00 μl (0.50 μl/side); NAc, AP = +1.30 mm, ML = ± 0.50 mm, DV = −4.80 mm, from bregma; flow rate of 0.10 μl/min and total volume of 0.60 μl (0.30 μl/side); BLA, AP = −1.80 mm, ML = ± 3.00 mm, DV = −4.80 mm from

bregma, flow rate of 0.10 μl/min and total volume of 0.60 μl (0.30 μl/side). An additional 5 min was allowed for diffusion and prevention of backflow. Behavioural tests or in vivo extracellular recordings were conducted 21 days after AAV injection.

For NAc cannula implantation, adult male C57BL/6 mice were anaesthetized and mounted onto a stereotaxic frame (KOPF, US). The skull surface was coated with Kerr phosphoric acid gel etchant (Kerr USA). First, a bilateral guide cannula was inserted into the NAc (co-ordinates: 1.4 mm anterior to bregma, 0.5 mm lateral to midline, and 3.8 mm ventral to dorsal). Then, adhesive (GLUMA, Germany) was applied onto the skull and cannula surface, and Resina fluida (Filtek Z350 XT 3 M, USA) was brushed on top with light curing for 45 s using a VALO curing light (Ultradent Products). Finally, dental cement was used to seal the cannula, and a dummy cannula was inserted into the guide cannula to maintain unobstructed cannula. After surgery, animals were individually housed and then allowed to recover for 21 days with daily handling. Mice were conscious, unrestrained and freely moving in their home cages during the microinjections. On the experimental day, a 33-G stainless-steel injector connected to a 5-μl syringe was inserted into the guide cannula and extended 1 mm beyond the tip of the guide cannula. CNO (900pmol/0.3μl/side) or vehicle was infused bilaterally over 2.5 min. The injector tips were held in place for an additional 5 min after the end of infusion to avoid backflow through the needle track. Behavioural tests were performed 45 min after microinjections.

4.5. Electrophysiology

Mice were anaesthetized with 4 % chloral hydrate (400 mg/kg, intraperitoneally). The core body temperature was sustained at 37 °C via a thermostatically controlled heating pad during the whole process. Nine electrode tracks (100 μm interval, grid pattern) were placed in the VTA (coordinates: 3.3–3.5 mm posterior to the bregma, 0.3–0.5 mm lateral to the midline, and 3.5–5.0 mm below the brain surface). Putative VTA dopamine and GABA neurons were identified using established electrophysiological criteria (dopamine neurons: unfiltered waveform duration >2.2 ms overall, start-to-trough waveform duration ≥1.1 ms with high-pass filter, firing rate range from 0.5 to 10 Hz (Tan et al., 2012; Grace and Bunney, 1983; Ungless and Grace, 2012); GABA neurons: waveform duration <1 ms, firing rate range from 5 to 60 Hz (Tan et al., 2012; Steffensen et al., 1998; Ko et al., 2018)). The recording time for each neuron was over 3 min. Three parameters of VTA dopamine neuron activity were measured: (1). the number of spontaneously active dopamine neurons per track; (2). average firing rate; and (3). average

percentage of burst firing, which is defined as the occurrence of two consecutive spikes with an inter-spike interval <80 ms, and the termination of a burst defined as two spikes with an inter-spike interval >160 ms (Grace and Bunney, 1983; Ungless and Grace, 2012).

4.6. Immunohistochemistry and cell counting

Mice were anaesthetized and transcardially perfused with cold PBS and 4 % paraformaldehyde (PFA) sequentially. Mouse brains were maintained in 4 % PFA at 4 °C overnight and then dehydrated in 30 % sucrose for 2 days. Coronal sections (40 μm) containing the target brain region were obtained using a freezing microtome (Leica, CM 1950). The sections were incubated in blocking buffer (10 % normal goat serum, 0.3 % Triton X-100) for 1 h at room temperature and then incubated with one or two primary antibodies overnight at 4 °C, followed by rinsing in PBS buffer and secondary antibody incubation for 4 h at room temperature. The sections were mounted with Gold antifade reagent containing DAPI (Invitrogen, Thermo Fisher Scientific). An Olympus FV10 microscope was used to capture images. Primary antibodies: c-Fos (CST, #2250) and tyrosine hydroxylase (TH) (ImmunoStar, #22941). The numbers of c-Fos, TH, GFP, mCherry and tdTomato positive cells were counted bilaterally by experimenters who were blind to the treatments. For each brain, the counting criteria for interested brain regions is described as follow: BLA, 3–4 slice, (every ninth section, from 0.94 mm to 2.18 posterior to bregma); NAc, 3–4 slice, (every fourth section, from 1.78 mm to 1.10 anterior to bregma); mPFC, 3–4 slice, (every third section, from 1.98 mm to 1.54 mm anterior to bregma); VTA, IPN, and SN, 3–4 slice, (every third section, from 3.16 mm to 3.64 posterior to bregma); DG, 3–4 slice, (every sixth section, from 1.46 mm to 2.54 posterior to bregma). For each brain, the number of immunopositive cells of interested brain regions of per section was calculated by dividing the total number of immunopositive cells in all selected sections by the number of selected sections. For co-immuno experiments, using the percentage of TH positive of tdTomato labelled cells in VTA (Fig. 4H) as an example, we divided the total number of co-immuno cells (TH+/tdTomato+) in VTA of all selected slices by the total number of tdTomato positive cells in VTA of all selected slices.

4.7. Behavioural procedures

4.7.1. Positive experience (sex reward) and neutral experience

On the experimental day, both groups mice were moved to a behavior room with dim lighting conditions and housed individually. After 4 h of habituation, each positive experience group male mice were exposed to oestrous female mice for 2 h. The estrous cycle was assessed by microscopic evaluation of vaginal smears. For neutral experience, each male mice were housed with fake toy mice for 2 h.

4.7.2. Sexual behaviors

These data were collected during the positive experience. The first 30 min was videotaped using an infrared camera. The mounting latency, total times and duration of male mice were measured.

4.7.3. Acute and chronic restraint stress

Mice were moved to a behavior room on the experimental day and housed individually. After 4 h of habituation, mice were exposed to 2 h of restraint stress. Control mice were housed individually in the behavior room for 6 h without any treatment. For chronic restraint stress treatment, stress group mice were subjected to 2 h of restraint for 15 consecutive days.

4.7.4. Female urine sniffing test (FUST)

The female urine sniffing test was performed as previously described (Malkesman et al., 2010). On the experimental day, mice were transferred to a dimly lit behavior room at least 4 h before beginning the experiment. The test procedure was as follows: 1.3-min exposure to the cotton tip dipped in water; 2.45-min interval; 3.3-min exposure to the cotton tip infused with fresh urine from female mice in the oestrus phase. The duration of female urine sniffing time was scored.

4.7.5. Sucrose preference test (SPT)

Mice were habituated to drinking water from two bottles for one week before beginning testing. On the experimental day, water was deprived for 3 h, and then two bottles were introduced (1 % sucrose and water). Mice had free choice of either drinking 1 % sucrose solution or water for 2 h after lights off during the dark cycle. Sucrose and water consumption were determined by measuring the weight changes. Sucrose preference was calculated as the ratio of the mass of sucrose consumed versus the total mass of sucrose and water consumed during the test.

4.7.6. Locomotor

This test was performed in SuperFlex open field cages (40 × 40 × 30 cm, Omnitech Electronics Inc., Columbus, OH), and mice were allowed 30 min free exploration under illuminated conditions. The total distance travelled was quantified using Fusion software (Omnitech Electronics Inc., Columbus, OH).

4.7.7. Statistical analyses

Statistical analysis was performed with graphpad prism software. Results are presented as mean ± standard error of mean (S.E.M.). Shapiro–Wilk test was used to test the normality and equal variance assumptions. For normally distributed data, two-tailed t tests were used to assess differences between two experimental groups with equal variance. For a two-sample comparison of means with unequal variances, two-tailed t tests with Welch's correction were used. For non-normally distributed data, Mann–Whitney U tests were performed to compare two groups. For multiple groups, two-way ANOVAs followed by Tukey's multiple comparisons test were used. $P < 0.05$ was considered statistically significant.

CRediT authorship contribution statement

Linshan Sun: Investigation. **Jingjing You:** Investigation, Funding acquisition, Writing – review & editing. **Fengjiao Sun:** Investigation. **Minghu Cui:** Investigation. **Jiangong Wang:** Investigation. **Wentao Wang:** Investigation. **Dan Wang:** Investigation. **Dunjiang Liu:** Investigation. **Zhicheng Xu:** Investigation. **Changyun Qiu:** Investigation. **Bin Liu:** Conceptualization, Funding acquisition, Supervision, Writing – original draft, Writing – review & editing. **Haijing Yan:** Conceptualization, Funding acquisition, Supervision, Writing – original draft, Writing – review & editing.

Declaration of competing interest

The authors declare that they have no known competing financial interests or personal relationships that could have appeared to influence the work reported in this paper.

Appendix A. Supplementary data

Supplementary data to this article can be found online at https://doi.org/10.1016/j.ynstr.2021.100370.

References

Akil, H., Gordon, J., Hen, R., Javitch, J., Mayberg, H., McEwen, B., Meaney, M.J., Nestler, E.J., 2018. Treatment resistant depression: a multi-scale, systems biology approach. Neurosci. Biobehav. Rev. 84, 272–288. https://doi.org/10.1016/j.neubiorev.2017.08.019.

Ambroggi, F., Ishikawa, A., Fields, H.L., Nicola, S.M., 2008. Basolateral amygdala neurons facilitate reward-seeking behavior by exciting nucleus accumbens neurons. Neuron 59 (4), 648–661. https://doi.org/10.1016/j.neuron.2008.07.004.

Antunes, G.F., Gouveia, F.V., Rezende, F.S., Seno, M., de Carvalho, M.C., de Oliveira, C. C., Dos Santos, L., de Castro, M.C., Kuroki, M.A., Teixeira, M.J., Otoch, J.P., Brandao, M.L., Fonoff, E.T., Martinez, R., 2020. Dopamine modulates individual differences in avoidance behavior: a pharmacological, immunohistochemical, neurochemical and volumetric investigation. Neurobiol. Stress 12, 100219. https://doi.org/10.1016/j.ynstr.2020.100219.

Baimel, C., Lau, B.K., Qiao, M., Borgland, S.L., 2017. Projection-target-defined effects of orexin and dynorphin on VTA dopamine neurons. Cell Rep. 18 (6), 1346–1355. https://doi.org/10.1016/j.celrep.2017.01.030.

Bath, K.G., Russo, S.J., Pleil, K.E., Wohleb, E.S., Duman, R.S., Radley, J.J., 2017. Circuit and synaptic mechanisms of repeated stress: perspectives from differing contexts, duration, and development. Neurobiol. Stress 7, 137–151. https://doi.org/10.1016/j.ynstr.2017.05.001.

Bayer, H.M., Glimcher, P.W., 2005. Midbrain dopamine neurons encode a quantitative reward prediction error signal. Neuron 47 (1), 129–141. https://doi.org/10.1016/j.neuron.2005.05.020.

Beier, K.T., Steinberg, E.E., DeLoach, K.E., Xie, S., Miyamichi, K., Schwarz, L., Gao, X.J., Kremer, E.J., Malenka, R.C., Luo, L., 2015. Circuit architecture of VTA dopamine neurons revealed by systematic input-output mapping. Cell 162 (3), 622–634. https://doi.org/10.1016/j.cell.2015.07.015.

Bergamini, G., Mechtersheimer, J., Azzinnari, D., Sigrist, H., Buerge, M., Dallmann, R., Freije, R., Kouraki, A., Opacka-Juffry, J., Seifritz, E., Ferger, B., Suter, T., Pryce, C.R., 2018. Chronic social stress induces peripheral and central immune activation, blunted mesolimbic dopamine function, and reduced reward-directed behaviour in mice. Neurobiol. Stress 8, 42–56. https://doi.org/10.1016/j.ynstr.2018.01.004.

Björklund, A., Dunnett, S.B., 2007. Dopamine neuron systems in the brain: an update. Trends Neurosci. 30 (5), 194–202. https://doi.org/10.1016/j.tins.2007.03.006.

Bocklisch, C., Pascoli, V., Wong, J.C., House, D.R., Yvon, C., de Roo, M., Tan, K.R., Lüscher, C., 2013. Cocaine disinhibits dopamine neurons by potentiation of GABA transmission in the ventral tegmental area. Science 341 (6153), 1521–1525. https://doi.org/10.1126/science.1237059.

Brischoux, F., Chakraborty, S., Brierley, D.I., Ungless, M.A., 2009. Phasic excitation of dopamine neurons in ventral VTA by noxious stimuli. Proc. Natl. Acad. Sci. U. S. A. 106 (12), 4894–4899. https://doi.org/10.1073/pnas.0811507106.

Britt, J.P., Benalioud, F., McDevitt, R.A., Stuber, G.D., Wise, R.A., Bonci, A., 2012. Synaptic and behavioural profile of multiple glutamatergic inputs to the nucleus accumbens. Neuron 76 (4), 790–803. https://doi.org/10.1016/j.neuron.2012.09.040.

Bromberg-Martin, E.S., Matsumoto, M., Hikosaka, O., 2010. Dopamine in motivational control: rewarding, aversive, and alerting. Neuron 68 (5), 815–834.

Budygin, E.A., Park, J., Bass, C.E., Grinevich, V.P., Bonin, K.D., Wightman, R.M., 2012. Aversive stimulus differentially triggers subsecond dopamine release in reward regions. Neuroscience 201, 331–337. https://doi.org/10.1016/j.neuroscience.2011.10.056.

Burdick, K.E., Braga, R.J., Gopin, C.B., Malhotra, A.K., 2014. Dopaminergic influences on emotional decision making in euthymic bipolar patients. Neuropsychopharmacology 39 (2), 274–282. https://doi.org/10.1038/npp.2013.177.

Cao, J.L., Covington 3rd, H.E., Friedman, A.K., Wilkinson, M.B., Walsh, J.J., Cooper, D. C., Nestler, E.J., Han, M.H., 2010. Mesolimbic dopamine neurons in the brain reward circuit mediate susceptibility to social defeat and antidepressant action. J. Neurosci. 30 (49), 16453–16458. https://doi.org/10.1523/JNEUROSCI.3177-10.2010.

Caseras, X., Lawrence, N.S., Murphy, K., Wise, R.G., Phillips, M.L., 2013. Ventral striatum activity in response to reward: differences between bipolar I and II disorders. Am. J. Psychiatr. 170 (5), 533–541. https://doi.org/10.1176/appi.ajp.2012.12020169.

Charara, A., Grace, A.A., 2003. Dopamine receptor subtypes selectively modulate excitatory afferents from the hippocampus and amygdala to rat nucleus accumbens neurons. Neuropsychopharmacology 28 (8), 1412–1421. https://doi.org/10.1038/sj.npp.1300220.

Coccurello, R., 2019. Anhedonia in depression symptomatology: appetite dysregulation and defective brain reward processing. Behav. Brain Res. 372, 112041. https://doi.org/10.1016/j.bbr.2019.112041.

Creed, M., Ntamati, N.R., Chandra, R., Lobo, M.K., Lüscher, C., 2016. Convergence of reinforcing and anhedonic cocaine effects in the ventral pallidum. Neuron 92 (1), 214–226. https://doi.org/10.1016/j.neuron.2016.09.001.

Dandekar, M.P., Fenoy, A.J., Carvalho, A.F., Soares, J.C., Quevedo, J., 2018. Deep brain stimulation for treatment-resistant depression: an integrative review of preclinical and clinical findings and translational implications. Mol. Psychiatr. 23 (5), 1094–1112. https://doi.org/10.1038/mp.2018.2.

Dautan, D., Souza, A.S., Huerta-Ocampo, I., Valencia, M., Assous, M., Witten, I.B., Deisseroth, K., Tepper, J.M., Bolam, J.P., Gerdjikov, T.V., Mena-Segovia, J., 2016. Segregated cholinergic transmission modulates dopamine neurons integrated in distinct functional circuits. Nat. Neurosci. 19 (8), 1025–1033. https://doi.org/10.1038/nn.4335.

Davis, K.L., Kahn, R.S., Ko, G., Davidson, M., 1991. Dopamine in schizophrenia: a review and reconceptualization. Am. J. Psychiatr. 148 (11), 1474–1486. https://doi.org/10.1176/ajp.148.11.1474.

de Jong, J.W., Afjei, S.A., Pollak Dorocic, I., Peck, J.R., Liu, C., Kim, C.K., Tian, L., Deisseroth, K., Lammel, S., 2019. A neural circuit mechanism for encoding aversive stimuli in the mesolimbic dopamine system. Neuron 101 (1), 133–151. https://doi.org/10.1016/j.neuron.2018.11.005 e7.

Di Ciano, P., Everitt, B.J., 2004. Direct interactions between the basolateral amygdala and nucleus accumbens core underlie cocaine-seeking behavior by rats. J. Neurosci. 24 (32), 7167–7173. https://doi.org/10.1523/JNEUROSCI.1581-04.2004.

Dobi, A., Margolis, E.B., Wang, H.L., Harvey, B.K., Morales, M., 2010. Glutamatergic and nonglutamatergic neurons of the ventral tegmental area establish local synaptic contacts with dopaminergic and nondopaminergic neurons. J. Neurosci. 30 (1), 218–229. https://doi.org/10.1523/JNEUROSCI.3884-09.2010.

Dunlop, B.W., Nemeroff, C.B., 2007. The role of dopamine in the pathophysiology of depression. Arch. Gen. Psychiatr. 64 (3), 327–337. https://doi.org/10.1001/archpsyc.64.3.327.

Duszkiewicz, A.J., McNamara, C.G., Takeuchi, T., Genzel, L., 2019. Novelty and dopaminergic modulation of memory persistence: a tale of two systems. Trends Neurosci. 42 (2), 102–114. https://doi.org/10.1016/j.tins.2018.10.002.

Engelhard, B., Finkelstein, J., Cox, J., Fleming, W., Jang, H.J., Ornelas, S., Koay, S.A., Thiberge, S.Y., Daw, N.D., Tank, D.W., Witten, I.B., 2019. Specialized coding of sensory, motor and cognitive variables in VTA dopamine neurons. Nature 570 (7762), 509–513. https://doi.org/10.1038/s41586-019-1261-9.

Eshel, N., Bukwich, M., Rao, V., Hemmelder, V., Tian, J., Uchida, N., 2015. Arithmetic and local circuitry underlying dopamine prediction errors. Nature 525 (7568), 243–246. https://doi.org/10.1038/nature14855.

Fabbri, C., Crisafulli, C., Calati, R., Albani, D., Forloni, G., Calabrò, M., Martines, R., Kasper, S., Zohar, J., Juven-Wetzler, A., Souery, D., Montgomery, S., Mendlewicz, J., Serretti, A., 2017. Neuroplasticity and second messenger pathways in antidepressant efficacy: pharmacogenetic results from a prospective trial investigating treatment resistance. Eur. Arch. Psychiatr. Clin. Neurosci. 267 (8), 723–735. https://doi.org/10.1007/s00406-017-0766-1.

Ferenczi, E.A., Zalocusky, K.A., Liston, C., Grosenick, L., Warden, M.R., Amatya, D., Katovich, K., Mehta, H., Patenaude, B., Ramakrishnan, C., Kalanithi, P., Etkin, A., Knutson, B., Glover, G.H., Deisseroth, K., 2016. Prefrontal cortical regulation of brainwide circuit dynamics and reward-related behavior. Science 351 (6268), aac9698. https://doi.org/10.1126/science.aac9698.

Fields, H.L., Hjelmstad, G.O., Margolis, E.B., Nicola, S.M., 2007. Ventral tegmental area neurons in learned appetitive behavior and positive reinforcement. Annu. Rev. Neurosci. 30, 289–316. https://doi.org/10.1146/annurev.neuro.30.051606.094341.

Floresco, S.B., 2015. The nucleus accumbens: an interface between cognition, emotion, and action. Annu. Rev. Psychol. 66, 25–52. https://doi.org/10.1146/annurev-psych-010213-115159.

Fogelson, D.L., Leuchter, A., 2017. Defining treatment-resistant depression. JAMA psychiatry 74 (7), 758–759. https://doi.org/10.1001/jamapsychiatry.2017.0967.

French, S.J., Totterdell, S., 2003. Individual nucleus accumbens-projection neurons receive both basolateral amygdala and ventral subicular afferents in rats. Neuroscience 119 (1), 19–31. https://doi.org/10.1016/s0306-4522(03)00150-7.

Garriock, H.A., Kraft, J.B., Shyn, S.I., Peters, E.J., Yokoyama, J.S., Jenkins, G.D., Reinalda, M.S., Slager, S.L., McGrath, P.J., Hamilton, S.P., 2010. A genomewide association study of citalopram response in major depressive disorder. Biol. Psychiatr. 67 (2), 133–138. https://doi.org/10.1016/j.biopsych.2009.08.029.

Gore, F., Schwartz, E.C., Brangers, B.C., Aladi, S., Stujenske, J.M., Likhtik, E., Russo, M. J., Gordon, J.A., Salzman, C.D., Axel, R., 2015. Neural representations of unconditioned stimuli in basolateral amygdala mediate innate and learned responses. Cell 162 (1), 134–145. https://doi.org/10.1016/j.cell.2015.06.027.

Grace, A.A., Bunney, B.S., 1983. Intracellular and extracellular electrophysiology of nigral dopaminergic neurons–3. Evidence for electrotonic coupling. Neuroscience 10 (2), 333–348. https://doi.org/10.1016/0306-4522(83)90137-9.

Guillin, O., Abi-Dargham, A., Laruelle, M., 2007. Neurobiology of dopamine in schizophrenia. Int. Rev. Neurobiol. 78, 1–39. https://doi.org/10.1016/S0074-7742(06)78001-1.

Hadpech, S., Jinathep, W., Saoin, S., Thongkum, W., Chupradit, K., Yasamut, U., Moonmuang, S., Tayapiwatana, C., 2018. Impairment of a membrane-targeting protein translated from a downstream gene of a "self-cleaving" T2A peptide conjunction. Protein Expr. Purif. 150, 17–25. https://doi.org/10.1016/j.pep.2018.05.002.

Halbout, B., Marshall, A.T., Azimi, A., Liljeholm, M., Mahler, S.V., Wassum, K.M., Ostlund, S.B., 2019. Mesolimbic dopamine projections mediate cue-motivated reward seeking but not reward retrieval in rats. Elife 8, e43551. https://doi.org/10.7554/eLife.43551.

Hauser, T.U., Eldar, E., Dolan, R.J., 2017. Separate mesocortical and mesolimbic pathways encode effort and reward learning signals. Proc. Natl. Acad. Sci. Unit. States Am. 114 (35), E7395–E7404. https://doi.org/10.1073/pnas.1705643114.

Heymann, G., Jo, Y.S., Reichard, K.L., McFarland, N., Chavkin, C., Palmiter, R.D., Soden, M.E., Zweifel, L.S., 2020. Synergy of distinct dopamine projection populations in behavioural reinforcement. Neuron 105 (5), 909–920. https://doi.org/10.1016/j.neuron.2019.11.024 e5.

Horowitz, L.F., Montmayeur, J.P., Echelard, Y., Buck, L.B., 1999. A genetic approach to trace neural circuits. Proc. Natl. Acad. Sci. Unit. States Am. 96 (6), 3194–3199. https://doi.org/10.1073/pnas.96.6.3194.

Howard, C.D., Li, H., Geddes, C.E., Jin, X., 2017. Dynamic nigrostriatal dopamine biases action selection. Neuron 93 (6), 1436–1450. https://doi.org/10.1016/j.neuron.2017.02.029 e8.

Hyman, S.E., Malenka, R.C., 2001. Addiction and the brain: the neurobiology of compulsion and its persistence. Nat. Rev. Neurosci. 2 (10), 695–703. https://doi.org/10.1038/35094560.

Ilango, A., Kesner, A.J., Keller, K.L., Stuber, G.D., Bonci, A., Ikemoto, S., 2014. Similar roles of substantia nigra and ventral tegmental dopamine neurons in reward and aversion. J. Neurosci. 34 (3), 817–822. https://doi.org/10.1523/JNEUROSCI.1703-13.2014.

Kaufling, J., Girard, D., Maitre, M., Leste-Lasserre, T., Georges, F., 2017. Species-specific diversity in the anatomical and physiological organisation of the BNST-VTA pathway. Eur. J. Neurosci. 45 (9), 1230–1240. https://doi.org/10.1111/ejn.13554.

Kiening, K., Sartorius, A., 2013. A new translational target for deep brain stimulation to treat depression. EMBO Mol. Med. 5 (8), 1151–1153. https://doi.org/10.1002/emmm.201302947.

Kim, J., Pignatelli, M., Xu, S., Itohara, S., Tonegawa, S., 2016. Antagonistic negative and positive neurons of the basolateral amygdala. Nat. Neurosci. 19 (12), 1636–1646. https://doi.org/10.1038/nn.4414.

Ko, M.Y., Jang, E.Y., Lee, J.Y., Kim, S.P., Whang, S.H., Lee, B.H., Kim, H.Y., Yang, C.H., Cho, H.J., Gwak, Y.S., 2018. The role of ventral tegmental area gamma-aminobutyric acid in chronic neuropathic pain after spinal cord injury in rats. J. Neurotrauma 35 (15), 1755–1764. https://doi.org/10.1089/neu.2017.5381.

Koob, G.F., Le Moal, M., 2001. Drug addiction, dysregulation of reward, and allostasis. Neuropsychopharmacology 24 (2), 97–129. https://doi.org/10.1016/S0893-133X(00)00195-0.

Kumar, P., Goer, F., Murray, L., Dillon, D.G., Beltzer, M.L., Cohen, A.L., Brooks, N.H., Pizzagalli, D.A., 2018. Impaired reward prediction error encoding and striatal-midbrain connectivity in depression. Neuropsychopharmacology 43 (7), 1581–1588. https://doi.org/10.1038/s41386-018-0032-x.

Lammel, S., Lim, B.K., Ran, C., Huang, K.W., Betley, M.J., Tye, K.M., Deisseroth, K., Malenka, R.C., 2012. Input-specific control of reward and aversion in the ventral tegmental area. Nature 491 (7423), 212–217. https://doi.org/10.1038/nature11527.

Lammel, S., Tye, K.M., Warden, M.R., 2014. Progress in understanding mood disorders: optogenetic dissection of neural circuits. Gene Brain Behav. 13 (1), 38–51. https://doi.org/10.1111/gbb.12049.

Lavin, A., Nogueira, L., Lapish, C.C., Wightman, R.M., Phillips, P.E., Seamans, J.K., 2005. Mesocortical dopamine neurons operate in distinct temporal domains using multimodal signaling. J. Neurosci. 25 (20), 5013–5023. https://doi.org/10.1523/JNEUROSCI.0557-05.2005.

LeGates, T.A., Kvarta, M.D., Tooley, J.R., Francis, T.C., Lobo, M.K., Creed, M.C., Thompson, S.M., 2018. Reward behaviour is regulated by the strength of hippocampus-nucleus accumbens synapses. Nature 564 (7735), 258–262. https://doi.org/10.1038/s41586-018-0740-8.

Libbrecht, S., Van den Haute, C., Malinouskaya, L., Gijsbers, R., Baekelandt, V., 2017. Evaluation of WGA-Cre-dependent topological transgene expression in the rodent brain. Brain Struct. Funct. 222 (2), 717–733. https://doi.org/10.1007/s00429-016-1241-x.

Lintas, A., Chi, N., Lauzon, N.M., Bishop, S.F., Gholizadeh, S., Sun, N., Tan, H., Laviolette, S.R., 2011. Identification of a dopamine receptor-mediated opiate reward memory switch in the basolateral amygdala-nucleus accumbens circuit. J. Neurosci. 31 (31), 11172–11183. https://doi.org/10.1523/JNEUROSCI.1781-11.2011.

Liu, D., Tang, Q.Q., Yin, C., Song, Y., Liu, Y., Yang, J.X., Liu, H., Zhang, Y.M., Wu, S.Y., Song, Y., Juarez, B., Ding, H.L., Han, M.H., Zhang, H., Cao, J.L., 2018. Brain-derived neurotrophic factor-mediated projection-specific regulation of depressive-like and nociceptive behaviors in the mesolimbic reward circuitry. Pain 159 (1), 175. https://doi.org/10.1097/j.pain.0000000000001083.

Lohani, S., Martig, A.K., Underhill, S.M., DeFrancesco, A., Roberts, M.J., Rinaman, L., Amara, S., Moghaddam, B., 2018. Burst activation of dopamine neurons produces prolonged post-burst availability of actively released dopamine. Neuropsychopharmacology 43 (10), 2083–2092. https://doi.org/10.1038/s41386-018-0088-7.

Loureiro, M., Lüscher, C., 2018. An unusual suspect in cocaine addiction. EMBO Rep. 19 (9), e46743 https://doi.org/10.15252/embr.201846743.

Luo, Y.J., Li, Y.D., Wang, L., Yang, S.R., Yuan, X.S., Wang, J., Cherasse, Y., Lazarus, M., Chen, J.F., Qu, W.M., Huang, Z.L., 2018. Nucleus accumbens controls wakefulness by a subpopulation of neurons expressing dopamine D1 receptors. Nat. Commun. 9 (1), 1576. https://doi.org/10.1038/s41467-018-03889-3.

Lüscher, C., 2016. The emergence of a circuit model for addiction. Annu. Rev. Neurosci. 39, 257–276. https://doi.org/10.1146/annurev-neuro-070815-013920.

MacAskill, A.F., Little, J.P., Cassel, J.M., Carter, A.G., 2012. Subcellular connectivity underlies pathway-specific signaling in the nucleus accumbens. Nat. Neurosci. 15 (12), 1624–1626. https://doi.org/10.1038/nn.3254.

Maldonado-Irizarry, C.S., Swanson, C.J., Kelley, A.E., 1995. Glutamate receptors in the nucleus accumbens shell control feeding behavior via the lateral hypothalamus. J. Neurosci. 15 (10), 6779–6788. https://doi.org/10.1523/JNEUROSCI.15-10-06779.1995.

Malkesman, O., Scattoni, M.L., Paredes, D., Tragon, T., Pearson, B., Shaltiel, G., Chen, G., Crawley, J.N., Manji, H.K., 2010. The female urine sniffing test: a novel approach for assessing reward-seeking behavior in rodents. Biol. Psychiatry 67 (9), 864–871. https://doi.org/10.1016/j.biopsych.2009.10.018.

Margolis, E.B., Lock, H., Hjelmstad, G.O., Fields, H.L., 2006. The ventral tegmental area revisited: is there an electrophysiological marker for dopaminergic neurons? J. Physiol. 577 (Pt 3), 907–924. https://doi.org/10.1113/jphysiol.2006.117069.

Martínez-Rivera, A., Hao, J., Tropea, T.F., Giordano, T.P., Kosovsky, M., Rice, R.C., Lee Martínez-Rivera, A., Hao, J., Tropea, T.F., Giordano, T.P., Kosovsky, M., Rice, R.C., Lee, A., Huganir, R.L., Striessnig, J., Addy, N.A., Han, S., Rajadhyaksha, A.M., 2017. Enhancing VTA Cav1.3 L-type Ca2+ channel activity promotes cocaine and mood-related behaviors via overlapping AMPA receptor mechanisms in the nucleus accumbens. Mol. Psychiatr. 22 (12), 1735–1745. https://doi.org/10.1038/mp.2017.9.

Matsui, A., Williams, J.T., 2011. Opioid-sensitive GABA inputs from rostromedial tegmental nucleus synapse onto midbrain dopamine neurons. J. Neurosci. 31 (48), 17729–17735. https://doi.org/10.1523/JNEUROSCI.4570-11.2011.

Matsui, A., Jarvie, B.C., Robinson, B.G., Hentges, S.T., Williams, J.T., 2014. Separate GABA afferents to dopamine neurons mediate acute action of opioids, development of tolerance, and expression of withdrawal. Neuron 82 (6), 1346–1356. https://doi.org/10.1016/j.neuron.2014.04.030.

Matsumoto, M., Hikosaka, O., 2009. Two types of dopamine neuron distinctly convey positive and negative motivational signals. Nature 459 (7248), 837–841. https://doi.org/10.1038/nature08028.

Mayberg, H.S., Lozano, A.M., Voon, V., McNeely, H.E., Seminowicz, D., Hamani, C., Schwalb, J.M., Kennedy, S.H., 2005. Deep brain stimulation for treatment-resistant depression. Neuron 45 (5), 651–660. https://doi.org/10.1016/j.neuron.2005.02.014.

McLaughlin, I., Dani, J.A., De Biasi, M., 2017. The medial habenula and interpeduncular nucleus circuitry is critical in addiction, anxiety, and mood regulation. J. Neurochem. 142 (Suppl. 2), 130–143. https://doi.org/10.1111/jnc.14008. Suppl 2.

Mohebi, A., Pettibone, J.R., Hamid, A.A., Wong, J.T., Vinson, L.T., Patriarchi, T., Tian, L., Kennedy, R.T., Berke, J.D., 2019. Dissociable dopamine dynamics for learning and motivation. Nature 570 (7759), 65–70. https://doi.org/10.1038/s41586-019-1235-y.

Morales, M., Margolis, E.B., 2017. Ventral tegmental area: cellular heterogeneity, connectivity and behaviour. Nat. Rev. Neurosci. 18 (2), 73–85. https://doi.org/10.1038/nrn.2016.165.

Nair-Roberts, R.G., Chatelain-Badie, S.D., Benson, E., White-Cooper, H., Bolam, J.P., Ungless, M.A., 2008. Stereological estimates of dopaminergic, GABAergic and glutamatergic neurons in the ventral tegmental area, substantia nigra and retrorubral field in the rat. Neuroscience 152 (4), 1024–1031. https://doi.org/10.1016/j.neuroscience.2008.01.046.

Nestler, E.J., Carlezon Jr., W.A., 2006. The mesolimbic dopamine reward circuit in depression. Biol. Psychiatr. 59 (12), 1151–1159. https://doi.org/10.1016/j.biopsych.2005.09.018.

Nestler, E.J., Lüscher, C., 2019. The molecular basis of drug addiction: linking epigenetic to synaptic and circuit mechanisms. Neuron 102 (1), 48–59. https://doi.org/10.1016/j.neuron.2019.01.016.

Ostlund, S.B., LeBlanc, K.H., Kosheleff, A.R., Wassum, K.M., Maidment, N.T., 2014. Phasic mesolimbic dopamine signaling encodes the facilitation of incentive motivation produced by repeated cocaine exposure. Neuropsychopharmacology 39 (10), 2441–2449. https://doi.org/10.1038/npp.2014.96.

Ostroumov, A., Thomas, A.M., Kimmey, B.A., Karsch, J.S., Doyon, W.M., Dani, J.A., 2016. Stress increases ethanol self-administration via a shift toward excitatory GABA signaling in the ventral tegmental area. Neuron 92 (2), 493–504. https://doi.org/10.1016/j.neuron.2016.09.029.

Pascoli, V., Terrier, J., Hiver, A., Lüscher, C., 2015. Sufficiency of mesolimbic dopamine neuron stimulation for the progression to addiction. Neuron 88 (5), 1054–1066. https://doi.org/10.1016/j.neuron.2015.10.017.

Pessiglione, M., Seymour, B., Flandin, G., Dolan, R.J., Frith, C.D., 2006. Dopamine-dependent prediction errors underpin reward-seeking behaviour in humans. Nature 442 (7106), 1042–1045. https://doi.org/10.1038/nature05051.

Pignatelli, M., Bonci, A., 2015. Role of dopamine neurons in reward and aversion: a synaptic plasticity perspective. Neuron 86 (5), 1145–1157. https://doi.org/10.1016/j.neuron.2015.04.015.

Pignatelli, M., Bonci, A., 2018. Spiraling connectivity of NAc-VTA circuitry. Neuron 97 (2), 261–262. https://doi.org/10.1016/j.neuron.2017.12.046.

Pizzagalli, D.A., Holmes, A.J., Dillon, D.G., Goetz, E.L., Birk, J.L., Bogdan, R., Dougherty, D.D., Iosifescu, D.V., Rauch, S.L., Fava, M., 2009. Reduced caudate and nucleus accumbens response to rewards in unmedicated individuals with major depressive disorder. Am. J. Psychiatr. 166 (6), 702–710. https://doi.org/10.1176/appi.ajp.2008.08081201.

Polter, A.M., Barcomb, K., Tsuda, A.C., Kauer, J.A., 2018. Synaptic function and plasticity in identified inhibitory inputs onto VTA dopamine neurons. Eur. J. Neurosci. 47 (10), 1208–1218. https://doi.org/10.1111/ejn.13879.

Popescu, A.T., Zhou, M.R., Poo, M.M., 2016. Phasic dopamine release in the medial prefrontal cortex enhances stimulus discrimination. Proc. Natl. Acad. Sci. Unit. States Am. 113 (22), E3169–E3176. https://doi.org/10.1073/pnas.1606098113.

Ramirez, S., Liu, X., MacDonald, C.J., Moffa, A., Zhou, J., Redondo, R.L., Tonegawa, S., 2015. Activating positive memory engrams suppresses depression-like behaviour. Nature 522 (7556), 335–339. https://doi.org/10.1038/nature14514.

Rappaport, B.I., Kandala, S., Luby, J.L., Barch, D.M., 2020. Brain reward system dysfunction in adolescence: current, cumulative, and developmental periods of depression. Am. J. Psychiatr. 177 (8), 754–763. https://doi.org/10.1176/appi.ajp.2019.19030281.

Robinson, S.A., Hill-Smith, T.E., Lucki, I., 2019. Buprenorphine prevents stress-induced blunting of nucleus accumbens dopamine response and approach behavior to food reward in mice. Neurobiol. Stress 11, 100182. https://doi.org/10.1016/j.ynstr.2019.100182.

Russo, S.J., Nestler, E.J., 2013. The brain reward circuitry in mood disorders. Nat. Rev. Neurosci. 14 (9), 609–625. https://doi.org/10.1038/nrn3381.

Saddoris, M.P., Cacciapaglia, F., Wightman, R.M., Carelli, R.M., 2015. Differential dopamine release dynamics in the nucleus accumbens core and shell reveal complementary signals for error prediction and incentive motivation. J. Neurosci. 35 (33), 11572–11582. https://doi.org/10.1523/JNEUROSCI.2344-15.2015.

Schultz, W., 2006. Behavioural theories and the neurophysiology of reward. Annu. Rev. Psychol. 57, 87–115. https://doi.org/10.1146/annurev.psych.56.091103.070229.

Sesack, S.R., Grace, A.A., 2010. Cortico-Basal Ganglia reward network: microcircuitry. Neuropsychopharmacology 35 (1), 27–47. https://doi.org/10.1038/npp.2009.93.

Setlow, B., Holland, P.C., Gallagher, M., 2002. Disconnection of the basolateral amygdala complex and nucleus accumbens impairs appetitive pavlovian second-order conditioned responses. Behav. Neurosci. 116 (2), 267–275. https://doi.org/10.1037//0735-7044.116.2.267.

Simmons, D.V., Petko, A.K., Paladini, C.A., 2017. Differential expression of long-term potentiation among identified inhibitory inputs to dopamine neurons. J. Neurophysiol. 118 (4), 1998–2008. https://doi.org/10.1152/jn.00270.2017.

Soares-Cunha, C., Coimbra, B., David-Pereira, A., Borges, S., Pinto, L., Costa, P., Soares-Cunha, C., Coimbra, B., David-Pereira, A., Borges, S., Pinto, L., Costa, P., Sousa, N., Rodrigues, A.J., 2016. Activation of D2 dopamine receptor-expressing neurons in the nucleus accumbens increases motivation. Nat. Commun. 7, 11829. https://doi.org/10.1038/ncomms11829.

Steffensen, S.C., Svingos, A.L., Pickel, V.M., Henriksen, S.J., 1998. Electrophysiological characterization of GABAergic neurons in the ventral tegmental area. J. Neurosci. 18 (19), 8003–8015. https://doi.org/10.1523/JNEUROSCI.18-19-08003.1998.

Strauss, G.P., Gold, J.M., 2012. A new perspective on anhedonia in schizophrenia. Am. J. Psychiatr. 169 (4), 364–373. https://doi.org/10.1176/appi.ajp.2011.11030447.

Stuber, G.D., Sparta, D.R., Stamatakis, A.M., van Leeuwen, W.A., Hardjoprajitno, J.E., Cho, S., Tye, K.M., Kempadoo, K.A., Zhang, F., Deisseroth, K., Bonci, A., 2011. Excitatory transmission from the amygdala to nucleus accumbens facilitates reward seeking. Nature 475 (7356), 377–380. https://doi.org/10.1038/nature10194.

Tan, K.R., Yvon, C., Turiault, M., Mirzabekov, J.J., Doehner, J., Labouèbe, G., Deisseroth, K., Tye, K.M., Lüscher, C., 2012. GABA neurons of the VTA drive conditioned place aversion. Neuron 73 (6), 1173–1183. https://doi.org/10.1016/j.neuron.2012.02.015.

Tervo, D.G., Hwang, B.Y., Viswanathan, S., Gaj, T., Lavzin, M., Ritola, K.D., Lindo, S., Michael, S., Kuleshova, E., Ojala, D., Huang, C.C., Gerfen, C.R., Schiller, J., Dudman, J.T., Hantman, A.W., Looger, L.L., Schaffer, D.V., Karpova, A.Y., 2016. A designer AAV variant permits efficient retrograde Access to projection neurons. Neuron 92 (2), 372–382. https://doi.org/10.1016/j.neuron.2016.09.021.

Ungless, M.A., Magill, P.J., Bolam, J.P., 2004. Uniform inhibition of dopamine neurons in the ventral tegmental area by aversive stimuli. Science 303 (5666), 2040–2042. https://doi.org/10.1126/science.1093360.

Ungless, M.A., Grace, A.A., 2012. Are you or aren't you? Challenges associated with physiologically identifying dopamine neurons. Trends Neurosci. 35 (7), 422–430. https://doi.org/10.1016/j.tins.2012.02.003.

Usuda, I., Tanaka, K., Chiba, T., 1998. Efferent projections of the nucleus accumbens in the rat with special reference to subdivision of the nucleus: biotinylated dextran amine study. Brain Res. 797 (1), 73–93. https://doi.org/10.1016/s0006-8993(98)00359-x.

van Zessen, R., Phillips, J.L., Budygin, E.A., Stuber, G.D., 2012. Activation of VTA GABA neurons disrupts reward consumption. Neuron 73 (6), 1184–1194. https://doi.org/10.1016/j.neuron.2012.02.016.

Vong, L., Ye, C., Yang, Z., Choi, B., Chua Jr., S., Lowell, B.B., 2011. Leptin action on GABAergic neurons prevents obesity and reduces inhibitory tone to POMC neurons. Neuron 71 (1), 142–154. https://doi.org/10.1016/j.neuron.2011.05.028.

Vrieze, E., Pizzagalli, D.A., Demyttenaere, K., Hompes, T., Sienaert, P., de Boer, P., Schmidt, M., Claes, S., 2013. Reduced reward learning predicts outcome in major depressive disorder. Biol. Psychiatr. 73 (7), 639–645. https://doi.org/10.1016/j.biopsych.2012.10.014.

Wassum, K.M., Ostlund, S.B., Loewinger, G.C., Maidment, N.T., 2013. Phasic mesolimbic dopamine release tracks reward seeking during expression of Pavlovian-to-instrumental transfer. Biol. Psychiatr. 73 (8), 747–755. https://doi.org/10.1016/j.biopsych.2012.12.005.

Wassum, K.M., Izquierdo, A., 2015. The basolateral amygdala in reward learning and addiction. Neurosci. Biobehav. Rev. 57, 271–283. https://doi.org/10.1016/j.neubiorev.2015.08.017.

Wickersham, I.R., Lyon, D.C., Barnard, R.J., Mori, T., Finke, S., Conzelmann, K.K., Young, J.A., Callaway, E.M., 2007. Monosynaptic restriction of transsynaptic tracing from single, genetically targeted neurons. Neuron 53 (5), 639–647. https://doi.org/10.1016/j.neuron.2007.01.033.

Willuhn, I., Wanat, M.J., Clark, J.J., Phillips, P.E., 2010. Dopamine signaling in the nucleus accumbens of animals self-administering drugs of abuse. Curr Top Behav Neurosci 3, 29–71. https://doi.org/10.1007/7854_2009_27.

Wittmann, B.C., Schott, B.H., Guderian, S., Frey, J.U., Heinze, H.J., Düzel, E., 2005. Reward-related FMRI activation of dopaminergic midbrain is associated with enhanced hippocampus-dependent long-term memory formation. Neuron 45 (3), 459–467. https://doi.org/10.1016/j.neuron.2005.01.010.

Yang, H., de Jong, J.W., Tak, Y., Peck, J., Bateup, H.S., Lammel, S., 2018. Nucleus accumbens subnuclei regulate motivated behavior via direct inhibition and disinhibition of VTA dopamine subpopulations. Neuron 97 (2), 434–449. https://doi.org/10.1016/j.neuron.2017.12.022 e4.

Yoshihara, Y., Mizuno, T., Nakahira, M., Kawasaki, M., Watanabe, Y., Kagamiyama, H., Jishage, K., Ueda, O., Suzuki, H., Tabuchi, K., Sawamoto, K., Okano, H., Noda, T., Mori, K., 1999. A genetic approach to visualization of multisynaptic neural pathways using plant lectin transgene. Neuron 22 (1), 33–41. https://doi.org/10.1016/s0896-6273(00)80676-5.

Zhang, X., Kim, J., Tonegawa, S., 2020. Amygdala reward neurons form and store fear extinction memory. Neuron 105 (6), 1077–1093. https://doi.org/10.1016/j.neuron.2019.12.025 e7.

Zhou, Z., Liu, X., Chen, S., Zhang, Z., Liu, Y., Montardy, Q., Tang, Y., Wei, P., Liu, N., Li, L., Song, R., Lai, J., He, X., Chen, C., Bi, G., Feng, G., Xu, F., Wang, L., 2019. A VTA GABAergic neural circuit mediates visually evoked innate defensive responses. Neuron 103 (3), 473–488. https://doi.org/10.1016/j.neuron.2019.05.027 e6.